The X-Ray Crystal Structure Determination of 5,6-Dibromonicotinic Acid and 5-Bromo,6-chloronicotinic Acid

Everly, Clarence A. Jr., Major
HQDA, MILPERCEN (DAPC-OPA-E)
200 Stovall Street
Alexandria, VA 22332

Final report, 27 August 1988

A thesis submitted to the University of Arkansas at Little Rock, Little Rock, Arkansas, in partial fulfillment of the requirements for the degree of Master of Science in Chemistry.

Unclassified
SECURITY CLASSIFICATION OF THIS PAGE

REPORT DOCUMENTATION PAGE

Form Approved
OMB No 0704-0188
Exp. Date Jun 30, 1986

1a. REPORT SECURITY CLASSIFICATION: Unclassified

1b. RESTRICTIVE MARKINGS:

2a. SECURITY CLASSIFICATION AUTHORITY:

2b. DECLASSIFICATION / DOWNGRADING SCHEDULE:

3. DISTRIBUTION / AVAILABILITY OF REPORT: Approved for public release; distribution is unlimited.

4. PERFORMING ORGANIZATION REPORT NUMBER(S):

5. MONITORING ORGANIZATION REPORT NUMBER(S):

6a. NAME OF PERFORMING ORGANIZATION: HQDA MILPERCEN DAPC-OPB-D

6b. OFFICE SYMBOL (If applicable):

7a. NAME OF MONITORING ORGANIZATION:

6c. ADDRESS (City, State, and ZIP Code):

7b. ADDRESS (City, State, and ZIP Code):

8a. NAME OF FUNDING / SPONSORING ORGANIZATION:

8b. OFFICE SYMBOL (If applicable):

9. PROCUREMENT INSTRUMENT IDENTIFICATION NUMBER:

8c. ADDRESS (City, State, and ZIP Code):

10. SOURCE OF FUNDING NUMBERS

PROGRAM ELEMENT NO.	PROJECT NO.	TASK NO.	WORK UNIT ACCESSION NO.

11. TITLE (Include Security Classification): The X-Ray Crystal Structure Determination of 5,6-Dibromonicotinic Acid and 5-Bromo,6-chloronicotinic Acid

12. PERSONAL AUTHOR(S): Everly, Clarence Albert

13a. TYPE OF REPORT	13b. TIME COVERED	14. DATE OF REPORT (Year, Month, Day)	15. PAGE COUNT
Final	FROM 87/05/29 TO 88/08/27	88/08/27	

16. SUPPLEMENTARY NOTATION:

17. COSATI CODES			18. SUBJECT TERMS (Continue on reverse if necessary and identify by block number)
FIELD	GROUP	SUB-GROUP	X-RAY Crystal Structure Determination

19. ABSTRACT (Continue on reverse if necessary and identify by block number)

For some years a large series of new and closely related dihalonicotinic acids, dihalonicotinamides, and dihalopicolines have been in the process of synthesis in the Chemistry Department at the University of Arkansas at Little Rock. The study of such a series often affords new insights into the nature of matter.

When it was observed that the three types of trisubstituted pyridines order themselves according to melting points, it was proposed that hydrogen bonding among molecules in the crystals of the acids and amides is an important intermolecular force which largely determines crystal structure.

Proof of this can be obtained only by crystal structure determinations. Consequently, the structure determinations of 5,6-dibromonicotinic acid and 5-bromo-6-chloro-nicotinic acid were undertaken. [YES] (over)

20. DISTRIBUTION / AVAILABILITY OF ABSTRACT
■ UNCLASSIFIED/UNLIMITED ☐ SAME AS RPT. ☐ DTIC USERS

21. ABSTRACT SECURITY CLASSIFICATION: Unclassified

22a. NAME OF RESPONSIBLE INDIVIDUAL	22b TELEPHONE (Include Area Code)	22c. OFFICE SYMBOL
Maj C.A. Everly		

DD FORM 1473, 84 MAR — 83 APR edition may be used until exhausted. All other editions are obsolete.

SECURITY CLASSIFICATION OF THIS PAGE
Unclassified

BIK 19. (cont)

Quite good structures have come out of the research, and these show hydrogen bonding in both cases. However, there is a difference in the types of hydrogen bonds between the two compounds studied. Some preliminary attempts to explain the gross differences between crystal structures have been made. Nevertheless, these explanations are only preliminary, and can be made truly correct only after crystal structures of other dihalonicotinic acids have been determined.

It is proposed that the next series of crystal structure determinations be those for 5,6-dichloronicotinic acid, 6-bromo-5-chloronicotinic acid, 5-bromo-6-fluoronicotinic acid, and 6-bromo-5-fluoronicotinic acid.

The X-Ray Structure Determination of 5,6-Dibromonicotinic Acid and of 5-Bromo-6-chloronicotinic Acid

A thesis submitted in partial fulfillment of the requirements for the degree of Master of Science

by

Clarence Albert Everly, Jr.

The University of Arkansas
at Little Rock
1988

Approved by:

Alcuin F. Fratiello — 26 Aug 1988
Advisor — Date

Frank L. Setliff

Richard M. Kliss

Ralph G. Wolf

An Abstract

For some years, a large series of new and closely related dihalonicotinic acids, dihalonicotinamides, and dihalopicolines have been in process of synthesis in the Chemistry Department at the University of Arkansas at Little Rock. The study of such a series often affords new insights into the nature of matter.

Therefore, when it was observed that the three types of trisubstituted pyridines order themselves according to melting points, it was proposed that hydrogen bonding among molecules in the crystals of the acids and amides is an important intermolecular force which largely determines crystal structure.

Proof of this can be obtained by crystal structure determinations. Consequently, the structure determinations of 5,6-dibromonicotinic acid and 5-bromo-6-chloronicotinic acid were undertaken.

Quite good structures have come out of the research, and these show hydrogen bonding in both cases. However, there is a difference in types of hydrogen bonds as between the two compounds studied. Some preliminary attempts to explain the gross differences between crystal structures have been made. Nevertheless, these explanations are only preliminary, and can be made truly correct only after crystal structures of other dihalonicotinic acids have been determined.

It is proposed that the next series of crystal

structure determinations be those for 5,6-dichloronicotinic acid, 6-bromo-5-chloronicotinic acid, 5-bromo-6-fluoronicotinic acid, and 6-bromo-5-fluoronicotinic acid.

Acknowledgements

The author wishes to express his appreciation and indebtedness to Professor A. F. Gremillion for his guidance throughout the course of this research. His eternal optimism, patience, and ability to see the positive side of all problems were an inspiration throughout the course of this work.

Several people have contributed their time and material to this project. Professor F. L. Setliff with his assistant Mr. Steve Rankin provided the compounds which were the basis for this research, and Mr. Norman Hynes was most helpful in procuring many scientific materials.

Finally, a special note of thanks to Professor A. W. Cordes from the University of Arkansas, Fayetteville, for the use of and instruction on the CAD 4 automatic diffractometer on the Fayetteville campus.

Table of Contents

I.	Introduction	1
II.	Crystal Growth of 5,6-Dibromonicotinic Acid and of 5-Bromo-6-chloronicotinic Acid	6
III.	Crystal Engineering	8
IV.	Collection of Experimental Data for 5,6-Dibromonicotinic Acid by the Weissenberg Method	10
V.	Interpretation of Photographic Film Record	17
VI.	Structure Determination of 5,6-Dibromonicotinic Acid	41
VII.	Structure Determination of 5-Bromo-6-chloronicotinic Acid	50
VIII.	Results	53
IX.	Discussion of Results	56
X.	Future Work	62
XI.	Tables	63
XII.	Bibliography	93

I. Introduction

A series of compounds of closely related structures, such as an homologous series, often offers a special basis for the study of chemical and/or physical properties that lead to some insight into the nature of matter. Such a series of compounds has been available for some years in the Chemistry Department of the University of Arkansas at Little Rock. The compounds were first prepared and characterized by the research group of Professor Lamar Setliff. The series consists of a relatively large number of trisubstituted pyridines (1-6). A schematic representation of the syntheses of this research is presented below. This scheme illustrates the rich source of trisubstituted pyridines that is to be found in the synthetic routes to the dihalonicotinic acids. More are available through syntheses of the corresponding acid amides.

The first thought that a study of this series might offer an opportunity to learn more of hydrogen bonding in solids (7) came when Professor A. F. Gremillion arranged twenty-two of these compounds in order of increasing melting point. It was observed that the dihalopicolines have melting points that fall below the melting points of the group of dihalonicotinic acids, and these fall largely below the group of melting points of the dihalonicotinamides. These facts are indicated in Table I.

In addition to hydrogen bonding, dispersion forces and permanent dipole/permanent dipole interactions are likely to be among the most important intermolecular forces between

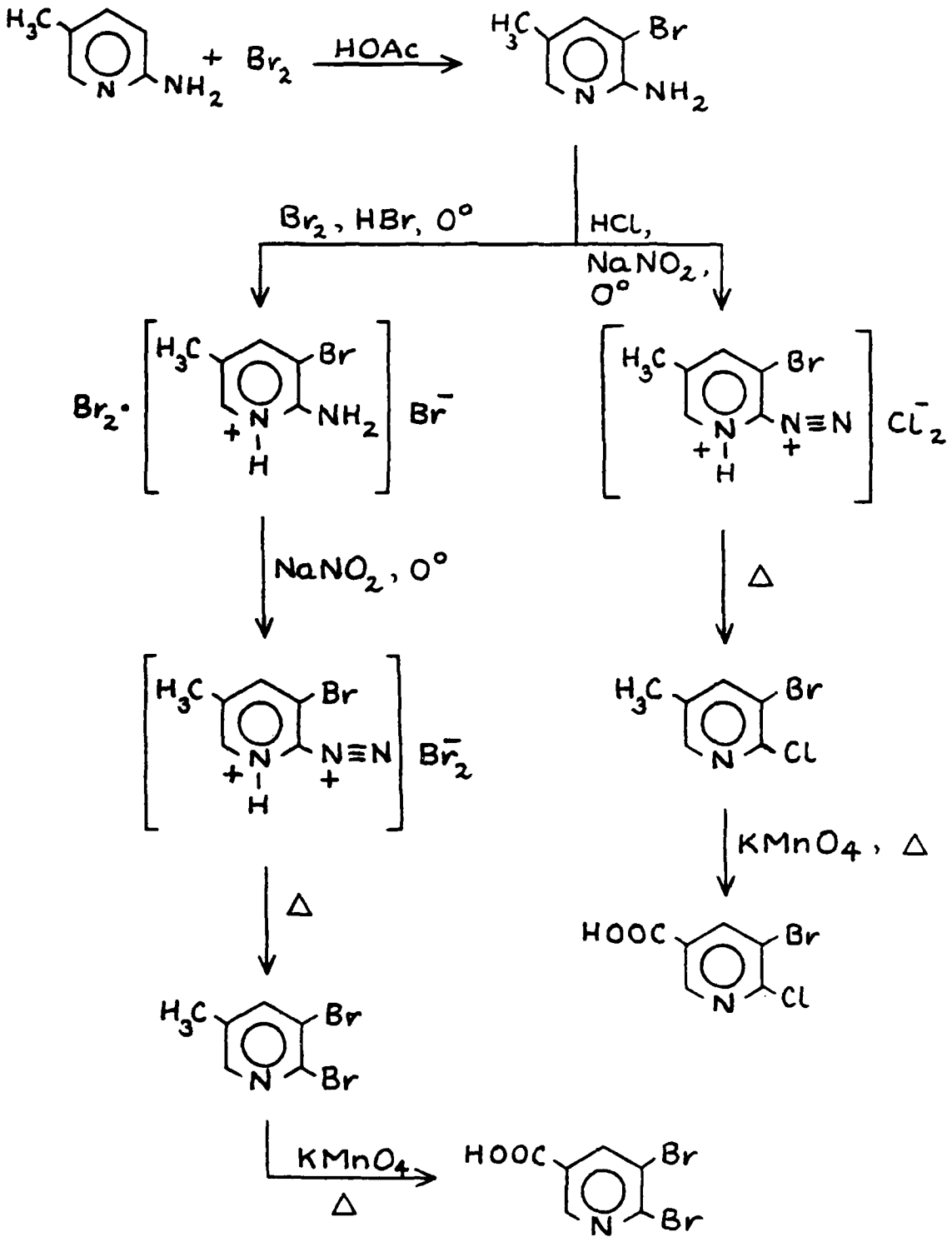
HOAc
Br2, HBr, 0°
HCl,
NaNO2,
0°
NaNO2, 0°
Δ
KMnO4, Δ
KMnO4
Δ

dihalonicotinic acid molecule pairs, and pairs of dihalonicotinamide molecules. Nevertheless, hydrogen bonding can be the overriding intermolecular force. In the case of molecular crystals (as in contrast with liquids), molecular shape may be important to the mode of packing of the molecular motif, and could have a strong modifying effect upon the influence of the intermolecular forces. The work of Kitaigorodskii (8) over many years has shown the importance of molecular shape in crystals of organic molecules. The case has been stated in a much more abbreviated form by Laing (9).

As an example, consider the 5,6-dibromonicotinic acid molecule with the structural formula given here.

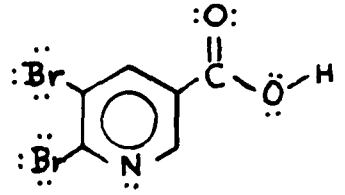

The electron pair acceptor in a hydrogen bond will be the hydrogen atom of the carboxylic acid group. But there are likely electron pair donors, and these are the nitrogen atom, the hydroxyl oxygen, and the carbonyl oxygen. A bromine atom seems much less likely as the electron donor than do those listed above. However, the shape of the molecule in the crystal may dictate the unexpected. Furthermore, there may be more than one kind of hydrogen bond. Only by crystal structure analysis can one locate the hydrogen bonds if they exist, and know the molecular packing

mode. This defines the grand problem at hand. The solution will involve many molecular compounds in which one has (a) a single electron pair acceptor and one or more donors, (b) a single electron pair donor and multiple acceptors, or (c) multiple electron donors in company with two or more acceptors. The importance of the hydrogen bond could not be more eloquently stated than to note that it is responsible for the double helix of the DNA molecule.

Once the program of research outlined above was agreed upon, preliminary work consisted of the acquisition of x-ray powder diffraction patterns for twenty - two trisubstituted pyridines. These were acquired with a Guinier camera which employs focused copper $K_{\alpha 1}$ radiation from a curved quartz crystal monochromator. Among these powder patterns are those of the compounds that are the subject of this thesis (10). The major problem with a powder pattern is that it could be one for a chemically pure substance that is nevertheless not phase pure. Polymorphism could be a problem. The only solution to this problem is found in the indexing of all lines in the powder pattern. The method of choice is that of Ito (11). Manual execution of this process is not recommended, so that until such time as a proper program for such calculations is available one should base the indexing on single crystal x-ray diffraction data. Even with the AIDS 83 program of the National Bureau of Standards (12) for application of Ito's method, single crystal data are welcome. However, the AIDS program will likely give a set of indices that are no better than the set of experimental

Bragg spacings with which it is provided.

The basis for this thesis has been the indexing of the necessary single crystal diffraction patterns, and the establishment of the space group symmetry for crystals of 5,6-dibromonicotinic acid, and 5-bromo-6-chloronicotinic acid grown very slowly from benzene solution. The additional basis has been the determination of the unit cell parameters. These bases constitute the x-ray crystallography of any crystalline compound which in turn is the springboard for the determination of the crystal structure.

The crystal structures of the two substituted nicotinic acids named above have also been determined so that in each case the hydrogen bonds have been located. The major intermolecular forces operating in crystals of these compounds have been identified.

II. Crystal Growth of 5,6 - Dibromonicotinic Acid and of 5-Bromo-6-chloronicotinic Acid

Each of the original materials provided by Professor F.L. Setliff was crystallized from a water-ethanol solution over a short period of time. This resulted in crystals that were insufficient in size (width and thickness) for use in single crystal x-ray studies. It was apparent that slow growth of appropriate crystals was necessary.

To assist in developing the appropriate technique and determine the best solvent for use in the crystal growth process, a model compound - *o*-chlorobenzoic acid - was selected on which several crystal growth techniques and solvents could be tested. The selection of this model was based on its ready availability, plentiful supply, and similarity to the target compound.

Experimentation indicated that an undisturbed saturated benzene solution, allowed to slowly evaporate, provided maximum crystal growth and crystal yield. Thereafter, all crystal growth was accomplished in this manner.

In order to achieve a state reasonably free from disturbance, the vessel containing the solution was floated in a large, water filled, glass dessicator which was placed on a six inch stack of computer paper covered with a piece of wood. The water served to maintain a nearly constant temperature for the crystal solution. The water and computer paper minimized vibrational disturbances.

The crystal solution consisted of 0.2503 grams of 5,6-dibromonicotinic acid dissolved in 121 ml of benzene in a

125 ml Erlenmeyer flask. The flask was fitted with a hollow plastic ring to which was attached a copper wire screen basket designed to hold the plastic ring firmly to the flask. A piece of filter paper was placed over the mouth of the flask to prevent debris from entering the solution. A piece of flat glass was placed on top of the filter paper to form a close seal and force slow evaporation. The entire flask - plastic ring construction was then floated in the dessicator.

After a period of 39 days of slow evaporation 0.2153 grams (86%) of the starting material was recovered as large crystals with well developed morphology. Large crystals of 5-bromo-6-chloronicotinic acid were grown in the same manner. After 120 days of slow evaporation, 0.2395 grams (95%) of the original 0.2525 grams was recovered.

III. Crystal Engineering

A satisfactory crystal for collecting single crystal x-ray diffraction data possesses uniform internal structure, and it has the proper size and shape (13).

To meet the first requirement the crystal should not be physically distorted or be twinned. The final crystals of 5,6-dibromonicotinic acid showed little twinning and that which was present was easily recognized. The crystals were well formed and transparent. To meet the second requirement, the shape and size of the crystal should be such that it is bathed in the x-ray beam at all times. The preferred size of the crystal is from 0.1mm to 0.3mm with the optimum usually being a crystal that is about 0.2mm x 0.2mm x 0.2mm.

The majority of the crystals grown were much larger than the optimum size, most notably in length and width. The major failing of the smaller crystals was in thickness. It was therefore necessary to engineer a large crystal to the desired dimensions through the use of a solvent saw.

A portion of the solvent saw consisted of a threaded spindle attached to a half cycle per minute electric motor. A two dimensional micromanipulator, made from two microscope stages, was attached to the base of the solvent saw and was designed to manipulate a piece of ashless filter paper soaked with solvent. The target crystal was attached to a goniometer head which was threaded onto the spindle of the solvent saw. As the crystal was rotated on the spindle, the solvent-soaked piece of filter paper was gently brought into contact with the crystal surface through the use of the

micromanipulator. In this manner, undesired portions of the crystal were dissolved away and the crystal shaped to the desired dimensions. The entire crystal engineering process was observed through a binocular microscope mounted above the crystal.

IV. Collection of Experimental Data for 5,6-Dibromonicotinic Acid by the Weissenberg Method

The most straightforward means of collecting crystallographic diffraction data is through photographic methods. These methods provide a view of the geometry and symmetry of the reciprocal lattice from which the direct cell constants and space group may be determined. Many types of cameras have been constructed for taking photographs of the reciprocal lattice. The camera used for the current studies is the Charles Supper model 9000 Weissenberg camera mounted on an Enraf Nonius Diffractus 581 x-ray generator. Both unfiltered and nickel filtered copper radiation were employed.

The crystal must be attached to a glass fiber. This is accomplished through the use of a one dimensional micromanipulator. A glass fiber of 3cm length and 0.2mm diameter was inserted into a pinhole in a 1/8 inch diameter brass pin. Apiezon Q was packed around the base of the glass fiber to hold it in place. The pin, with fiber in the vertical position, was fastened to the micromanipulator so that it could be moved up and down. The target crystal was then placed beneath the glass fiber atop an inverted glass funnel the end of which had been squared and filled with Apiezon. The glass fiber was lowered and the position of the funnel adjusted until the desired crystal axis was well aligned with the glass fiber. The entire operation was observed through a binocular microscope. Once alignment of the crystal and glass fiber was achieved, a tiny drop of 5

Minute Epoxy cement was placed on the lower tip of the glass fiber. The fiber was lowered gently until contact was made with the crystal. The crystal and glass fiber were left undisturbed for a 24 hour period to allow the epoxy cement to cure completely.

In single crystal diffraction studies, the crystal is mounted so that it can be aligned and centered in the camera (14). For this reason the brass pin with glass fiber and crystal was placed in an Enraf Nonius model 0516.908 eucentric goniometer head. The goniometer head has two arcs which allow the crystal to be tipped $\pm$ 15 degrees in each of two mutually perpendicular planes so that it may be exactly aligned with the axis of rotation of the crystal. In addition, the goniometer head has two sledges which allow centering (i.e. X Y plane adjustment) of the crystal on the goniometer head axis, and a Z component translation which allows for putting the crystal precisely in the path of the x-ray beam.

To make the initial alignment adjustments, the goniometer head was threaded onto the spindle of the Weissenberg camera. The crystal was slowly rotated by hand and gross adjustments made to the arcs of the goniometer head while observing the crystal through a telescope attached to the base of the camera. The necessary X, Y and Z adjustments were also made. Further alignment must be achieved by photographic methods.

Several types of photographs may be taken using the Charles Supper Weissenberg camera. Oscillation photographs

are used to further align the crystal and obtain initial information about crystal symmetry. No film translation occurs here.

In most cases the crystal is roughly aligned at the time of attachment to the glass fiber. This is shown on oscillation films by reciprocal lattice layer lines that are not exactly straight or that are tilted with respect to the center line of the film. These are clues to the misalignment of one of the crystallographic axes with the axis of rotation of the camera. Such misalignment is referred to the mutually perpendicular planes of the arcs of the goniometer head, one of which is initially set parallel to the incident x-ray beam. Initially, a crystal will be misaligned in both of these planes, and the resulting photograph will show a combination of the effect of misalignment in one plane and that for misalignment in the other plane.

The target crystal was continuously oscillated for one to two hours through a range of $\pm$ 15 degrees for each of a series of seven oscillation films. After each film, the appropriate adjustments were made to the arcs of the goniometer head. After the seventh film, the error in alignment was too small (less than 2 degrees) to make accurate adjustments using oscillation photographs. Final alignment must be made using normal mode zero-level Weissenberg photographs, i.e., those obtained while crystal oscillation is synchronized with film translation.

Oscillation photographs may also be used to obtain

initial information concerning crystal symmetry. An oscillation photograph may show one of the five following film symmetries: 1, $\bar{1}$, m_x, m_y, and mm (15). For example, the appearance of m_x symmetry on an oscillation film indicates a reciprocal lattice that has a mirror plane perpendicular to that axis of the direct lattice about which the crystal is rotated. Thus is the monoclinic crystal system indicated. The m_x film symmetry is the one of greatest practical value.

Rotation photographs taken with a Weissenberg camera are used to determine the repeat distance of the crystal axis of rotation. In a manner similar to the recording of oscillation photographs, the target crystal was continuously rotated through an arc of $\pm$ 351 degrees as the rotation photograph was taken after crystal alignment. The resulting reciprocal lattice layer lines are used to determine the axial repeat distance for the axis of rotation. The reciprocal lattice of a crystal is defined in Section V of this thesis.

Results obtained by this method are generally very precise. However, changes in the effective radius of the film cassette caused by the thickness of the film envelope plus film, and film shrinkage after development, may introduce substantial error (16). To minimize these effects, the film cassette and technique are standardized by measuring a substance of known axial spacing.

To accomplish the standardization, a normal mode rotation photograph is made of the target crystal. Without

removing the film from the film cassette, the film cassette is moved to the left or right a small distance (2mm). The target crystal is replaced by an aligned crystal of known axial spacing and a rotation photograph of the standard crystal is made on the same film. In this manner, the effective film radius can be determined for each film taken.

Normal mode reciprocal lattice zero-level Weissenberg photographs employing continuous translation of the film cassette, and a layer line screen allowing only reflections from the zero-level of the reciprocal lattice to reach the photographic film are used for several purposes: (1) final alignment of the target crystal, (2)location of the reciprocal lattice axial central lines and (3) determination of the reciprocal lattice primitive translations. At present, only final alignment of the target crystal will be discussed. In final alignment, exposures of fifty to ninety hours are not uncommon.

Translation of the film in zero-level Weissenberg photography results in central lattice line images that are straight and that form an angle τ with a horizontal line through the center of the film. A central lattice line is a film line made by a straight line of reciprocal lattice points that passes through the origin of the reciprocal lattice. For an ideally aligned crystal, the value of τ is 63.435 degrees. To further align a crystal, the angle that an observed central lattice line makes with the horizontal centerline of the film is measured and compared to the ideal

value. Corrections are made to both arcs of the goniometer head to bring the observed central lattice line to the ideal position.

Two normal mode reciprocal lattice zero level Weissenberg films were required to bring the target crystal to within 0.07 degrees of the ideal value for τ. A 0.06 degree correction is the limit of adjustment of the arcs on the goniometer head in use. The crystal was therefore considered aligned.

It is often convenient to have available Weissenberg photographs of upper levels of the reciprocal lattice. These films are needed for the calculation of interaxial angles as well as providing a complete picture of systematic absences for use in determination of the x-ray space group. The most advantageous means of obtaining these photographs is by the equi-inclination Weissenberg method.

In zero-level Weissenberg photographs the crystal is centered in the slit opening of the layer line screen by eye. For upper levels, the diffracted x-ray beam is not perpendicular to the axis of rotation. Therefore, the layer line screen must be shifted so that the reflections of the desired layer level pass through the layer line screen slit. In addition, the crystal, camera spindle, and film cassette carriage are inclined with respect to the x-ray beam so that reciprocal lattice points from the desired level intercept the sphere of reflection on one of its minor circles that is parallel to and of the same size as that upon which the origin of the reciprocal lattice falls.

It is important to note that more reciprocal lattice layers may be accessible using the equi - inclination method than with rotation photographs. Rotation photographs of the target crystal showed only the zero, first, and second layer levels. Using the equi - inclination Weissenberg method, photographs of the first, second, and third layer levels were obtained.

V. Interpretation of Photographic Film Record

Prior to the interpretation of x-ray diffraction photographs, it is essential that a thorough understanding of the reciprocal lattice and its relationship to the direct crystal lattice be obtained. Indeed, it is the reciprocal lattice and not the direct lattice that is being photographed and measured.

X-ray diffraction by a crystal may be thought of as reflection by sets of parallel planes in the crystal. Normally, it is very difficult to visualize the orientation and relationship between the planes in the direct lattice of a crystal. This is particularly true when the indices of these planes are not small and when the coordinate system defined by the unit cell edges is oblique. To simplify these problems, an imaginary geometric construction, the reciprocal lattice, is constructed from the direct crystal lattice (17). It is defined as follows: To each Bragg plane in the direct lattice a normal is drawn from the direct lattice origin. The length of each normal is such that it equals the reciprocal of the interplanar spacing, d_{hkl}, of the Bragg plane to which it is drawn (18). The point at the end of each normal is a reciprocal lattice point which corresponds to the set of planes to which its normal was drawn (Figure 1). The collection of these reciprocal lattice points constitutes the reciprocal lattice.

A mathematical definition of the reciprocal lattice is in order. Let the basis vectors of a rectilinear space be

Figure 1. Projection on the (010) plane of unit cell direct lattice planes with corresponding reciprocal lattice points, p, q, r, and s.

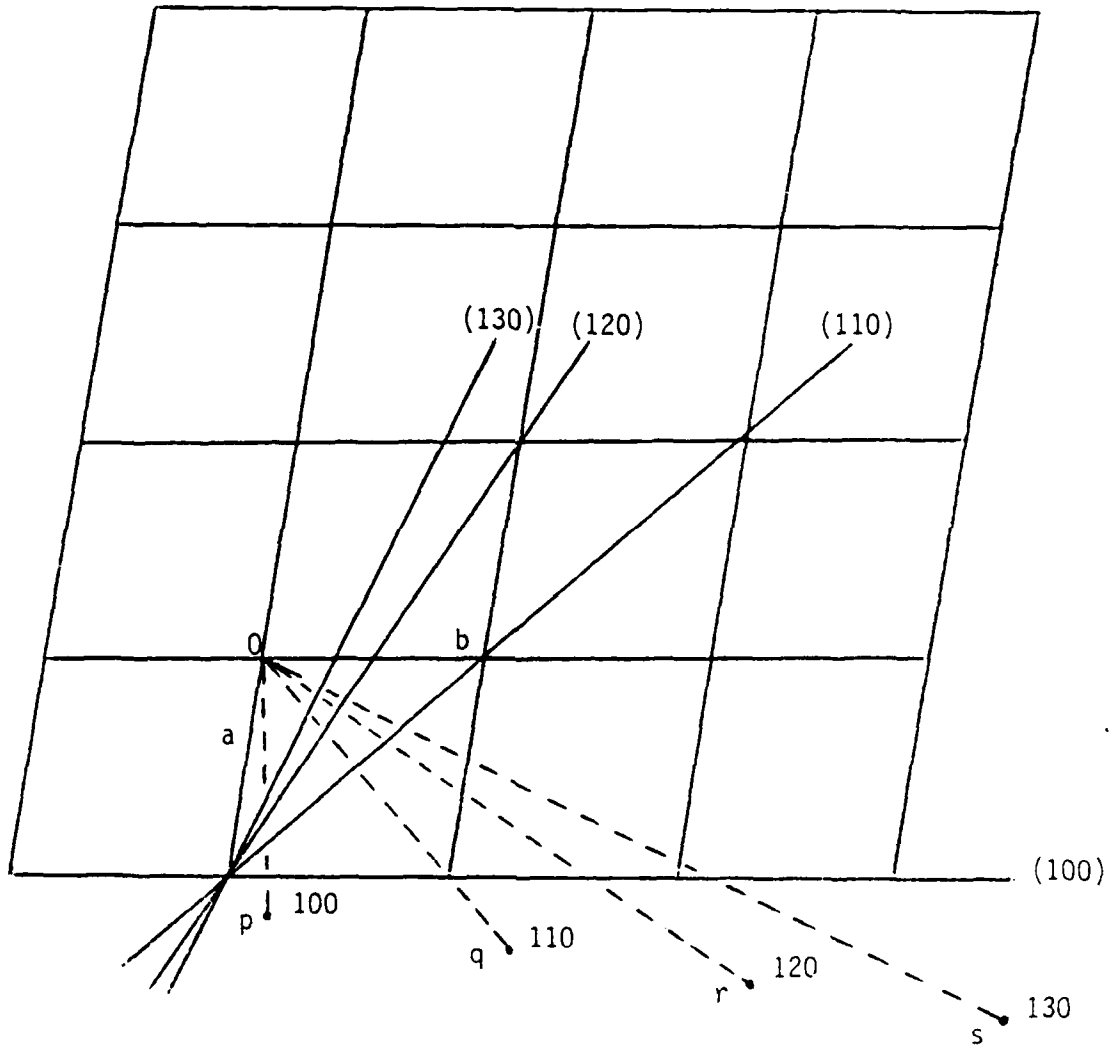

$\mathbf{a}_1$, $\mathbf{a}_2$, and $\mathbf{a}_3$. The rectilinear space corresponds to the space of the point lattice of a crystal, i.e., to the direct lattice. Further, let a_1, a_2 and a_3 be the vector magnitudes. A vector **U** in this space is then given by $\mathbf{U} = U^i \mathbf{a}_i$, where the Einstein summation convention is used, the U^i are the contravariant components of **U**, and the $\mathbf{a}_i$ are the covariant basis vectors. If **V** is another vector in this space, then $\mathbf{V} = V^i \mathbf{a}_i$, and $\mathbf{U} \cdot \mathbf{V} = U^i V^j \mathbf{a}_i \cdot \mathbf{a}_j$. Now, define $\mathbf{a}^j$ such that

$$\mathbf{a}_i \cdot \mathbf{a}^j = \delta_i^j = a_i \, a^j \cos(\mathbf{a}_i, \mathbf{a}^j) = 0$$

if $i \neq j$. Let the dot product be unity if $i = j$. The $\mathbf{a}^j$ represents the contravariant basis vectors for the reciprocal space corresponding to the reciprocal lattice. It follows that $\mathbf{a}^1$ is perpendicular to $\mathbf{a}_2$ and $\mathbf{a}_3$, that $\mathbf{a}^2$ is perpendicular to $\mathbf{a}_1$ and $\mathbf{a}_3$, and that $\mathbf{a}^3$ is perpendicular to $\mathbf{a}_2$ and $\mathbf{a}_3$. Consequently, $\mathbf{a}^1 = k(\mathbf{a}_2 \wedge \mathbf{a}_3)$. Multiplying by $\mathbf{a}_1$ gives

$$\mathbf{a}_1 \cdot \mathbf{a}^1 = k(\mathbf{a}_1 \cdot \mathbf{a}_2 \wedge \mathbf{a}_3) = 1 = \delta_1^1,$$

so that $k = 1/(\mathbf{a}_1 \cdot \mathbf{a}_2 \wedge \mathbf{a}_3) = 1/v$ where v is the volume of the unit cell of the direct lattice. We may then write

$$\mathbf{a}^1 = (\mathbf{a}_2 \wedge \mathbf{a}_3)/(\mathbf{a}_1 \cdot \mathbf{a}_2 \wedge \mathbf{a}_3),$$

$$\mathbf{a}^2 = (\mathbf{a}_3 \wedge \mathbf{a}_1)/(\mathbf{a}_1 \cdot \mathbf{a}_2 \wedge \mathbf{a}_3),$$

$\mathbf{a}^3 = (\mathbf{a}_1 \Lambda \mathbf{a}_2)/(\mathbf{a}_1 \cdot \mathbf{a}_2 \Lambda \mathbf{a}_3)$.

The two lattices are reciprocal to each other so that we may make the following statements: $\mathbf{a}^1 \perp \mathbf{a}_2$ and $\mathbf{a}_3$, $\mathbf{a}^2 \perp \mathbf{a}_3$ and $\mathbf{a}_1$, $\mathbf{a}^3 \perp \mathbf{a}_1$ and $\mathbf{a}_2$, $\mathbf{a}_1 \perp \mathbf{a}^2$ and $\mathbf{a}^3$, $\mathbf{a}_2 \perp \mathbf{a}^1$ and $\mathbf{a}^3$, $\mathbf{a}_3 \perp \mathbf{a}^1$ and $\mathbf{a}^2$. Most crystallographers use the direct lattice basis vectors **a**, **b**, **c** and reciprocal lattice basis vectors $\mathbf{a}^*$, $\mathbf{b}^*$, $\mathbf{c}^*$, i.e., $\mathbf{a}_1 = \mathbf{a}$, $\mathbf{a}_2 = \mathbf{b}$, $\mathbf{a}_3 = \mathbf{c}$, $\mathbf{a}^1 = \mathbf{a}^*$, $\mathbf{a}^2 = \mathbf{b}^*$, $\mathbf{a}^3 = \mathbf{c}^*$, $a = |\mathbf{a}|$, $b = |\mathbf{b}|$, $c = |\mathbf{c}|$, $a^* = |\mathbf{a}^*|$, $b^* = |\mathbf{b}^*|$, and $c^* = |\mathbf{c}^*|$. The most important property of the reciprocal lattice is that it allows a simple visualization of Bragg's law ($n\lambda = 2d_{hk\ell} \sin\theta_{hk\ell}$) in operation. Through the application of the reciprocal lattice, and Ewald's construction (Figure 2), we know that at the time of diffraction, mutually parallel reciprocal lattice planes exist parallel to the collimated x-ray beam of wavelength λ. If the incident x-ray beam passes through point O (Figure 2) - the origin of the reciprocal lattice - in the direction AO, a sphere of radius $1/\lambda$ (the sphere of reflection) with diameter AO can be constructed (17). Keeping the sphere fixed while rotating the crystal about a line through point C that is perpendicular to AO, the reciprocal lattice rotates simultaneously about a line through O that is also perpendicular to AO. While this occurs, the point P of the zero-level of the reciprocal lattice moves and eventually comes into contact with the surface of the sphere. Based on the definition of the

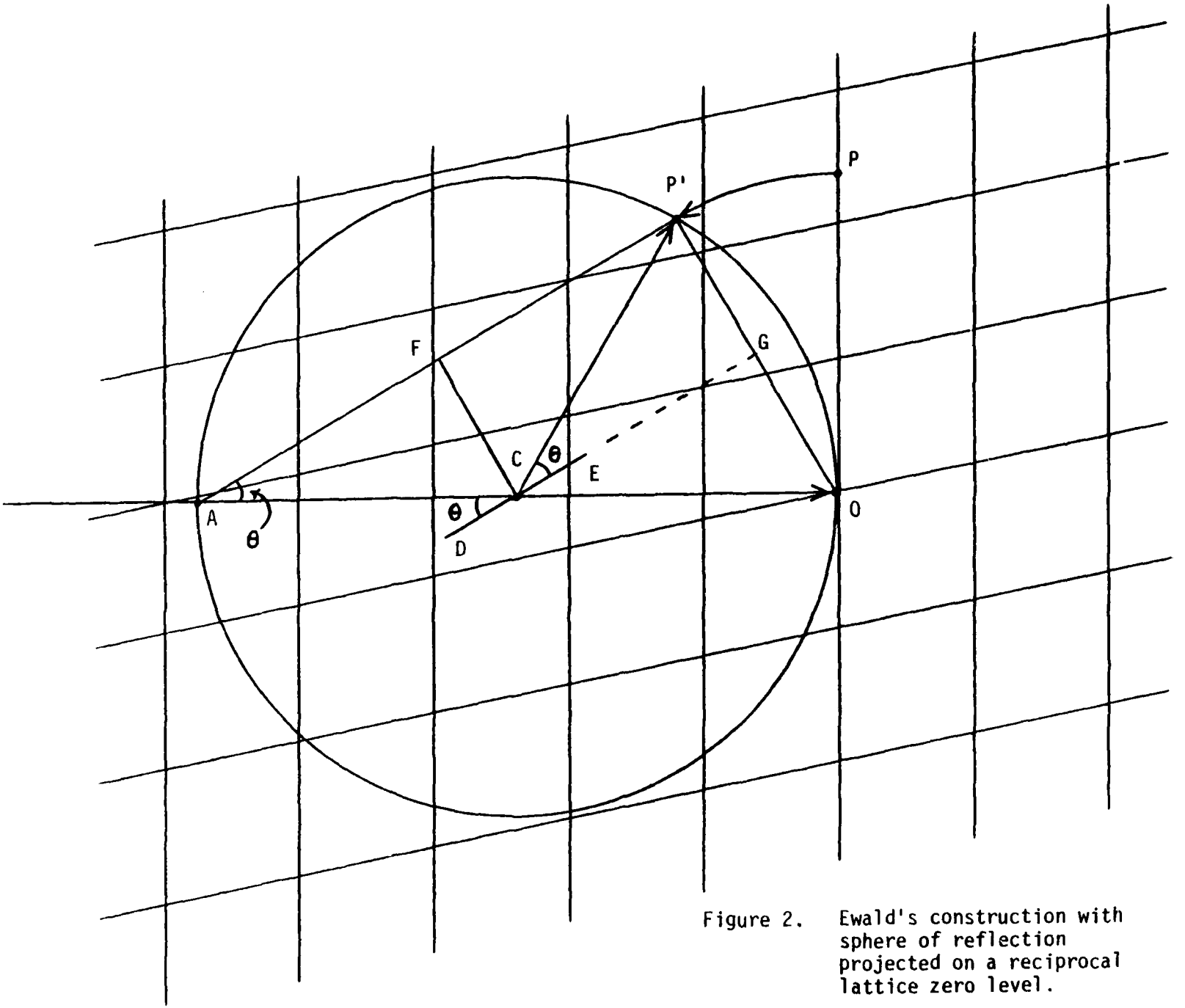

Figure 2. Ewald's construction with sphere of reflection projected on a reciprocal lattice zero level.

reciprocal lattice, OP' is $1/d_{hk\ell}$ $(=d^*_{hk\ell})$. The distance AO is $2/\lambda$ so that

$$\sin(P'AO) = OP'/AO = (1/d_{hk\ell})/(2/\lambda) = \lambda/2d_{hk\ell}$$

and Bragg's law is satisfied when point P comes into contact with the surface of the sphere of reflection. Those direct lattice planes corresponding to point P are in reflecting position. Let DE represent a set of Bragg planes parallel to AP'. CF is parallel to OP'. Then, $\sin(P'CG) = GP'/CP' = (1/2d_{hk\ell})/(1/\lambda)$ or $2d \sin(P'CG) = \lambda$ and $P'CG = \theta$. This allows a reflected beam of x-rays to dart from the crystal (located at C) along CP'. This matter is thoroughly discussed by M.J. Buerger (18) using vector methods.

The above general discussion is particularly suited to the interpretation of rotation photographs. In making rotation photographs, the crystal is mounted such that it rotates about one of the direct lattice axes. The direct lattice axis chosen is normally based on the morphology of the crystal. Its identity is not initially known. By the definition of the reciprocal lattice we know that one of the reciprocal lattice planes, parallel to the incident x-ray beam, bisects the sphere of reflection. This plane is called the zero-level reciprocal lattice plane. There are additional reciprocal lattice planes which are mutually parallel and are parallel to the zero-level plane. These are

perpendicular to the axis of rotation. The crystal is taken to be at the center of the sphere of reflection. As it rotates, the reciprocal lattice planes also rotate. As successive points of each of the reciprocal lattice planes come into contact with the sphere of reflection, the conditions for reflection are met. A beam of x-rays darts out and is recorded by a piece of cylindrical photographic film (Figure 3), the axis of which coincides with the rotation axis of the crystal. All diffracted beams associated with reciprocal lattice points common to a given reciprocal lattice level have the same height angle, ν. Height is distance along the film axis from the incident x-ray beam. The diffracted x-ray beams from a given reciprocal lattice upper level all intersect the film at the same height resulting in a series of spots that form a straight line (a reciprocal lattice layer line) when the film is unrolled.

Rotation photograph interpretation is now straightforward. The distance between the zero and nth layer lines on a rotation photograph is proportional to the perpendicular distance, ζ, between the zero and nth levels of reciprocal lattice points (19). ζ_n is then given by

$$\frac{\zeta_n}{1} = \frac{Y_n}{\sqrt{R^2+Y_n^2}} \sin \tan^{-1}\left(\frac{Y_n}{R}\right),$$

where Y_n is the distance measured on the film in millimeters from the zero to the nth layer line, and R is the true film

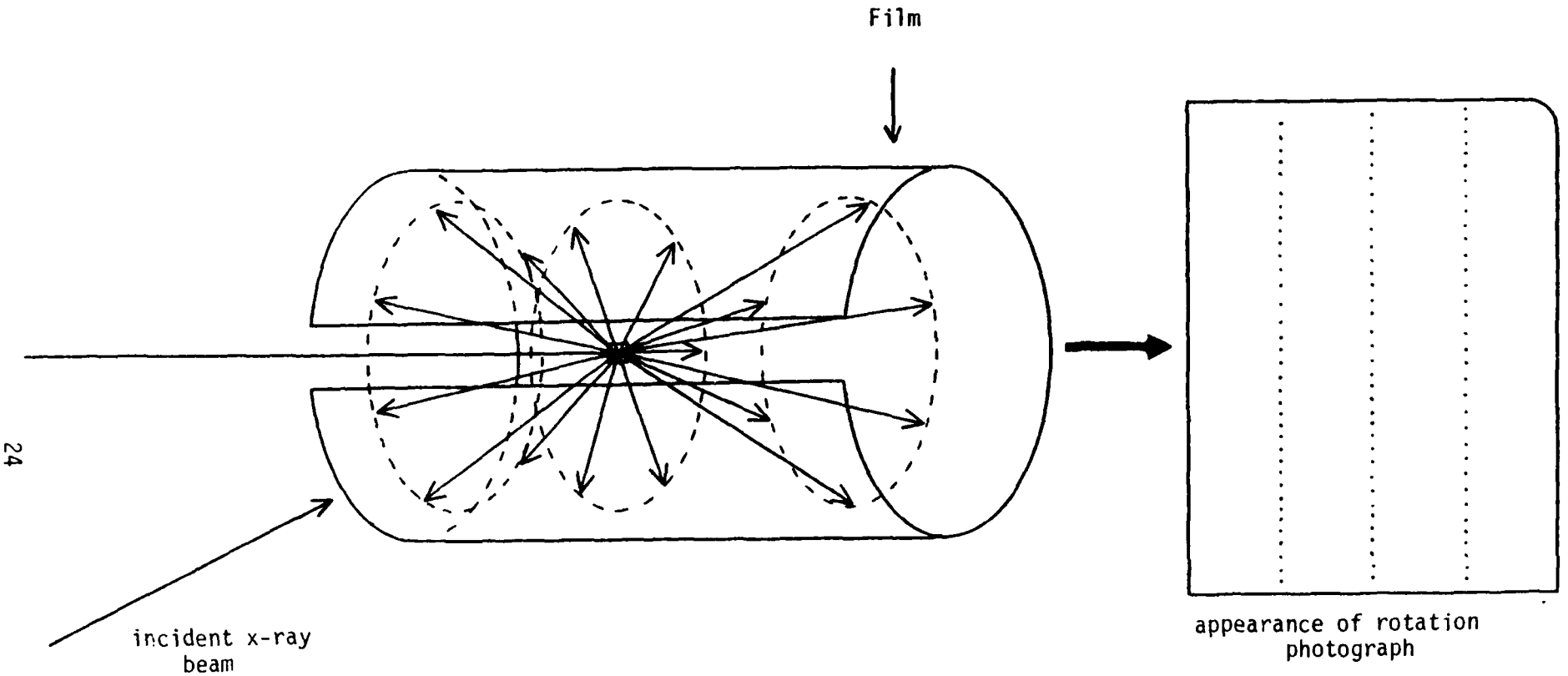

Figure 3. Recording reflections for a rotation photograph.

radius in millimeters. Film measurements were made using a Charles Supper Company film reader with a centimeter scale and vertical hairline capable of measuring to within 0.01 millimeters. The true film radius was determined by the means discussed earlier. After the exposure of the target crystal, an exposure of an appropriate NaCl crystal was made on the same film after a small film displacement. The literature value of 5.6396 Å + 0.00046 Å (d_{100} for NaCl with temperature correction) was used to calculate a true film diameter of 57.3 millimeters for this particular film. The nominal value for a film of undistorted diameter is 57.3 millimeters. No corrections were required.

Five reciprocal lattice layer lines for the target crystal were visible on the photograph taken, these being those with indices -2,-1,0,1,2. The distance, Y_n, was measured for the first and second layer levels and the value for ζ calculated for both (Table II).

Since the axis of rotation is perpendicular to the reciprocal lattice planes and therefore parallel to ζ, the repeat distance of these planes along the axis of rotation (19) (which is a direct lattice axis) is given by

$$r = \frac{\lambda}{\zeta_1} = \frac{n\lambda}{\sin \tan^{-1}(Y_n/R)}.$$

The λ (= 1.5418 Å) is the wavelength of the intensity weighted $K_{\alpha 1}/K_{\alpha 2}$ doublet. The experimental value of the direct lattice spacing along the axis of rotation was

determined to be 3.98 Å.

An early rotation photograph showed what appeared to be mirror symmetry. This led to the suspicion that perhaps the crystal belonged to one of the systems that could have a mirror symmetry element. The possibility that the rotation axis was an n-fold axis was tested with a series of oscillation photographs taken at steps of rotation azimuth of $(360^{o}/n)m$, where $n \geqslant m$, $m=1,2,3,\ldots$, and $n=6,4$ and 3 in succession. These photographs revealed no mirror symmetry, nor were any two of these photographs identical. This indicated that no axis of rotation of order higher than two coincided with the axis of rotation of the crystal. This also tended to eliminate the orthorhombic system. Further determination of the system to which the target crystal belonged was made from Weissenberg films.

As indicated earlier, Weissenberg photographs employ a moving film cassette with translation being parallel to the axis of rotation. In addition, a layer line screen is utilized to photograph only that reciprocal lattice layer level desired.

A central lattice line within a given reciprocal lattice level is one that passes through the origin of the level. The origin of the level is the origin of the lattice if the level is the zero-level. Of the many central lines of the level, the two having the greatest density of points are taken as axes of the level. The axis lines of the zero-level have diffraction patterns that are straight lines inclined

at 63.435 degrees to the film center line. The mutually parallel noncentral lattice lines crossing a single axis line of this level have a diffraction pattern that is a set of "concentric" festoons, each of which has Weissenberg distorted mirror symmetry about the straight line for one of the level axes. This is the basis for interpretation of Weissenberg zero-level films.

The first problem at hand is to determine which reciprocal lattice axes are present on a Weissenberg film from a crystal of unknown space group in an unspecified orientation. The best way to accomplish this is through a consideration of symmetry in the reciprocal lattice.

Two parallel central lattice lines were observed on the zero-level Weissenberg film of the target crystal, each of which corresponds to one of the axis lines of the level (Figure 4). It was also noted that mirror symmetry was present across the center of the film as well as across each of the two central lattice lines. In light of this symmetry, a strong case can be made for the monoclinic crystal system.

Two cases must be considered when discussing the monoclinic reciprocal lattice: (1) the rotation axis is b, or (2) the rotation axis is either a or c. The selection of the b axis as the axis of rotation would require that earlier oscillation photographs show mirror symmetry perpendicular to the rotation axis and that no mirror symmetry across central lattice lines be present (20). This is clearly not the case. The rotation axis is therefore

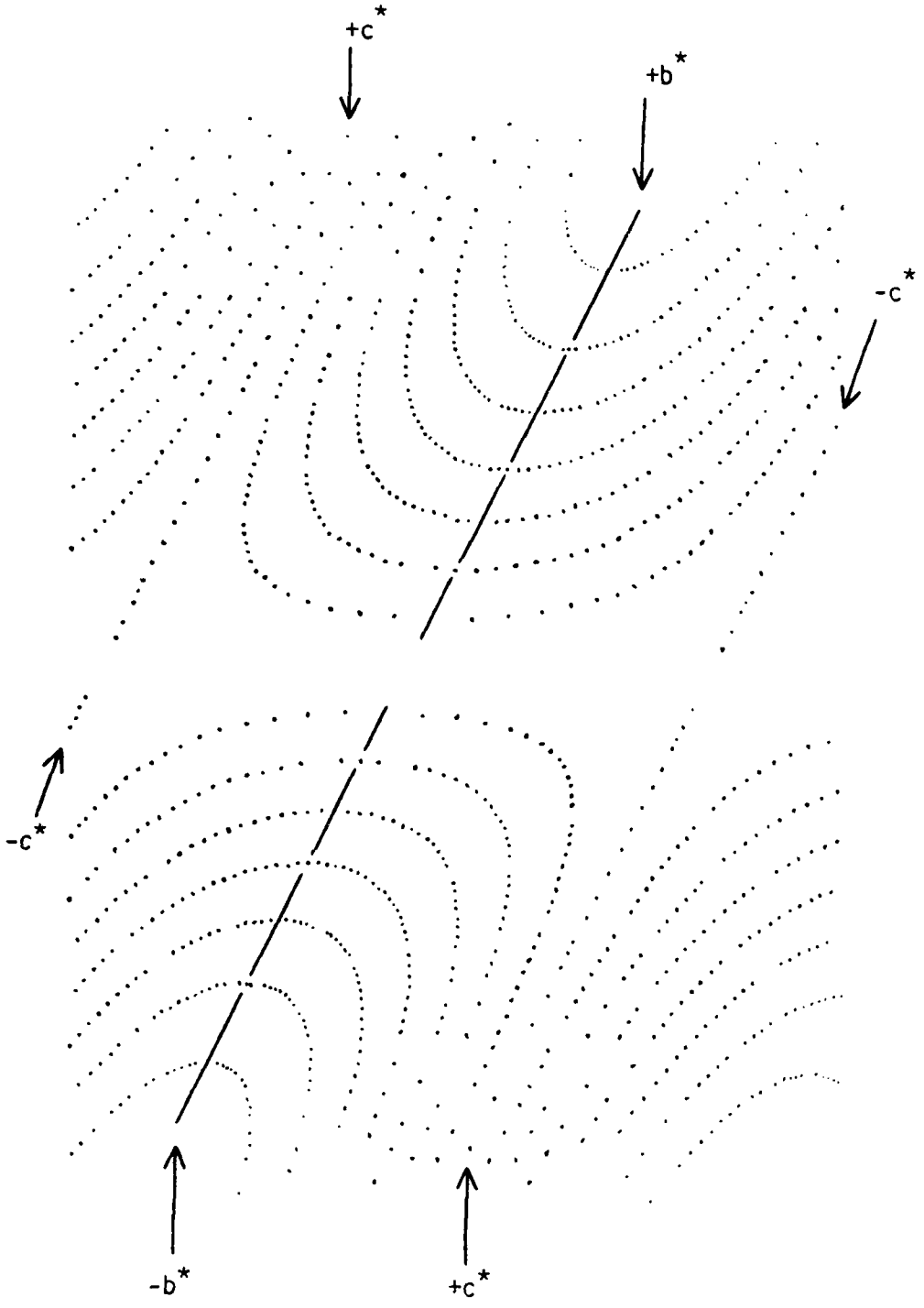

Figure 4. Replication of zero-level Weissenberg photograph depicting (a) central lattice lines, (b) noncentral lattice lines.

either a or c. For our purposes, c was selected as the axis of rotation. This means that the two central lattice lines taken on the Weissenberg film correspond to the a^* and b^* reciprocal lattice axes. The b^* axis is a 2-fold axis in the reciprocal lattice and the plane perpendicular to it containing the a^* axis is a mirror plane (20). The effect of a two-fold axis on two points lying in the same plane is that of a mirror. This requires that the central lattice lines corresponding to the a^* and b^* reciprocal lattice axes appear as mirror lines as was observed on the zero-level Weissenberg film of the target crystal. Since no mirror plane was observed perpendicular to the rotation axis (from earlier oscillation films), the symmetry conditions for the monoclinic system are satisfied. It remains now to determine which of the central lattice lines observed on the zero-level Weissenberg film corresponds to a^* and which corresponds to b^*. This must be accomplished through the use of upper-level Weissenberg films. The mounting of the crystal on the glass fiber so that the rotation axis was a or c was a matter of happenstance and of good fortune.

Previously, it was stated that in addition to alignment of the crystal and location of the reciprocal lattice axial lines, zero-level Weissenberg films are used to determine the axial repeat distance along the reciprocal lattice axes depicted on the zero-level film.

The axial repeat distance determination for zero-level Weissenberg films is similar to that for rotation

photographs. The perpendicular distance ($2Y_n$) between two corresponding axis line reflections, one above and one below the center line of the film, is proportional to the distance (ξ) from the same point to the origin of the reciprocal lattice (21). The distance ξ is then given by

$$\xi_n = 2 \sin \frac{2Y_n}{4R} \times 57.3,$$

where R is the true film radius. As before, film distances were determined using a Charles Supper film reader, and a value of 57.3 millimeters was used for 2R. This resulted in a value of 6.27 Å for the b axial repeat distance, and a value of 30.84 Å for the a axial repeat distance.

Upper-level photographs are most advantageously made using the equi-inclination Weissenberg method. Here, the x-ray beam is tilted with respect to the crystal (Figure 5) through the angle μ. As required by Bragg's law, the origin O of the reciprocal lattice remains at the point of exit of the x-ray beam. If the amount of tilt, μ, is properly chosen, there will be a point where the rotation axis intercepts the sphere of reflection and through which one axis of an upper-level of the reciprocal lattice passes (22). That point (S in Figure 5) remains fixed as the reciprocal lattice rotates so that the reciprocal point row h01 is an axis line of the first-level and will appear in a Weissenberg film as a straight line. The origin of the

Figure 5. Equi - inclination experiment for the first reciprocal lattice upper-level of a monoclinic unit cell rotated on a direct lattice c - axis.

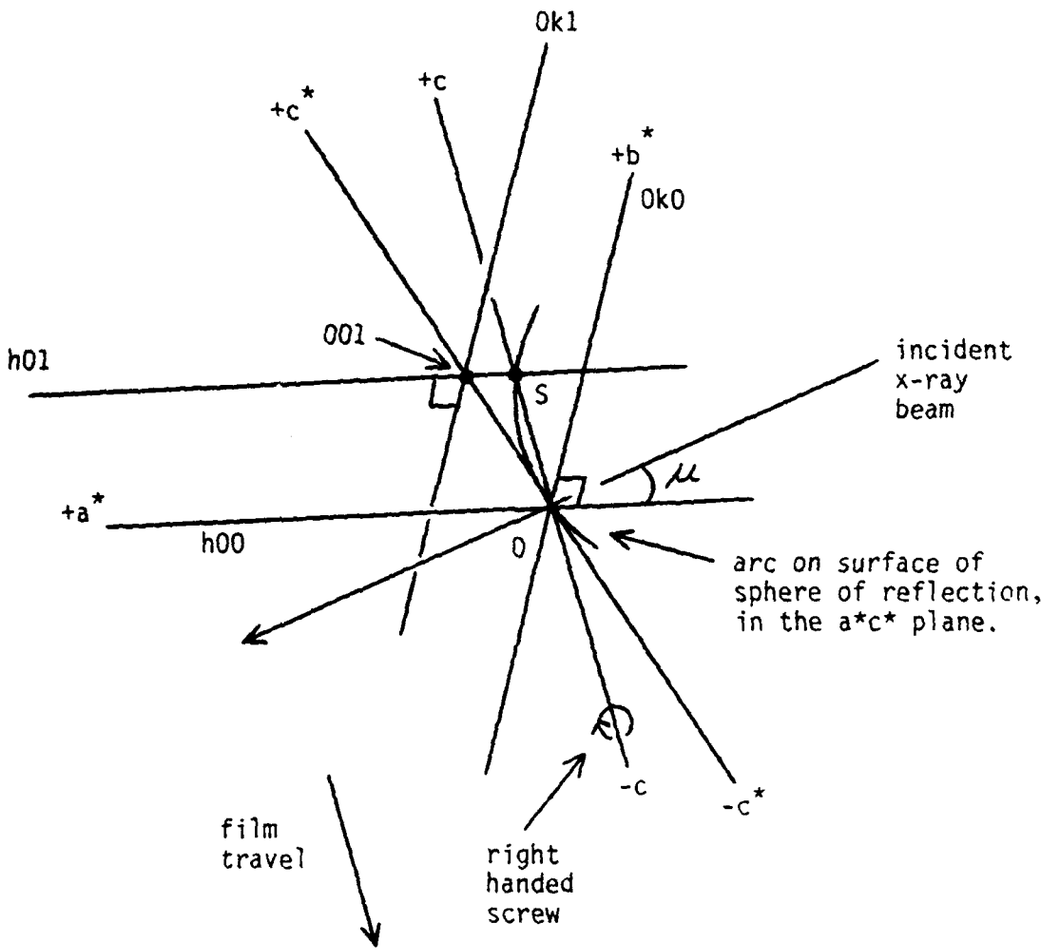

first-level is at 001. The second axis of this level (row 0k1) has none of its points at S so its diffraction pattern is a festoon which approximates to one with sharp corners.

The first-level equi-inclination Weissenberg film taken of the target crystal showed indeed a straight-line image of only one of the central lattice lines. This line corresponds to a^* on the zero-level Weissenberg film, and the other first-level axis corresponds to the b^* of the zero-level. Based on this assignment, the Weissenberg films can be indexed.

Prior to beginning the film indexing procedure, the cell constant β remained to be determined. To obtain the correct orientation of the reciprocal lattice on the upper-level photographs, the crystal had to be rotated 90 degrees. This would allow the observation and measurement of two symmetrical reflections on the nk1 festoon in the first-level film for use in the angular lag method for calculation of β. Determination of β in this fashion for the monoclinic case is based on the offset, from the origin, of two symmetrical reflections on the nk1 festoon in the first-level Weissenberg film or any other upper-level film where the appropriate festoon can be observed (23). This offset is relative to the position coordinate of the corresponding reflection on a zero-level film. The angle β is calculated using the relation

$$\beta = \tan^{-1}\left(-\frac{\zeta}{\xi_0}\tan\left\{\frac{c_2(z''-z')}{2}\right\}\right)$$

where ζ is the height of the reciprocal lattice upper-level being used (determined from previous rotation films), ξ_o is the zero-level film coordinate of the reflection being used, (z" - z') is the horizontal distance between the two symmetrical reflections used on the nth level film, and C_2 is a constant, 2^o/mm, for a camera of undistorted diameter. An upper-level Weissenberg film was taken for each of the first, second, and third layer levels and the value of β calculated from each. The first-level photograph yielded a value of 91.92 degrees, the second-level photograph a value of 91.90 degrees, and the third-level photograph a value of 91.95 degrees. The average of these three values was taken and the value of 91.92 degrees assigned to β (Table IV). In a later section of this thesis the use of the Enraf Nonius CAD 4 automatic diffractometer is described from which the value found is also 91.92 degrees.

Indexing, the process of assigning the appropriate hkℓ indices to each reflection on a given film, is started by determining which portion of each layer axis line and each noncentral lattice line is positive and which is negative. Central lattice lines that function as layer axes change sign as they cross the centerline of the film. Similarly, noncentral lattice lines change sign as they cross a layer axis line. By convention, crystallographic coordinate systems are chosen to be right handed and if one chooses the direction along the axis of rotation towards the tip of the crystal to be positive when viewed as from the direction of

the incident x-ray beam, the following relations are true: $+a^*$ is to the left of $+c^*$ or to the right of $+b^*$, and $+b^*$ is to right of $+c^*$ (20). In the case of a monoclinic crystal rotated about c, consultation of upper-level photographs is also required. Here, the shift in the festoons crossing the a^* axis observed by placing a first-level film over a zero-level film is in the positive direction. The shift observed by superimposing the appropriate films of the target crystal showed the a^* axis on the upper half of the film to be positive.

Two traces of the a^* central lattice line and one trace of the b^* central lattice line were present on the zero-level Weissenberg photograph of the target crystal. By the above convention, the upper portion of the right most a^* central lattice line was given a positive sign, the upper portion of the b^* central lattice line was given a positive sign, and the upper portion of the left most a^* central lattice line given a negative sign (Figure 4). By using the reciprocal lattice axial repeat distance to determine the index of the first observable reflection from the origin along both the b^* and a^* reciprocal lattice axes, the process of actually indexing the films was begun. The process is aided by the use of an accurate template for overlapping festoons that is available from the Institute of Physics and The Physical Society. See Figure 6. The reciprocal lattice axis lines on the template were aligned with the reciprocal lattice axis lines on the film. This

Figure 6. Weissenberg film indexing template.

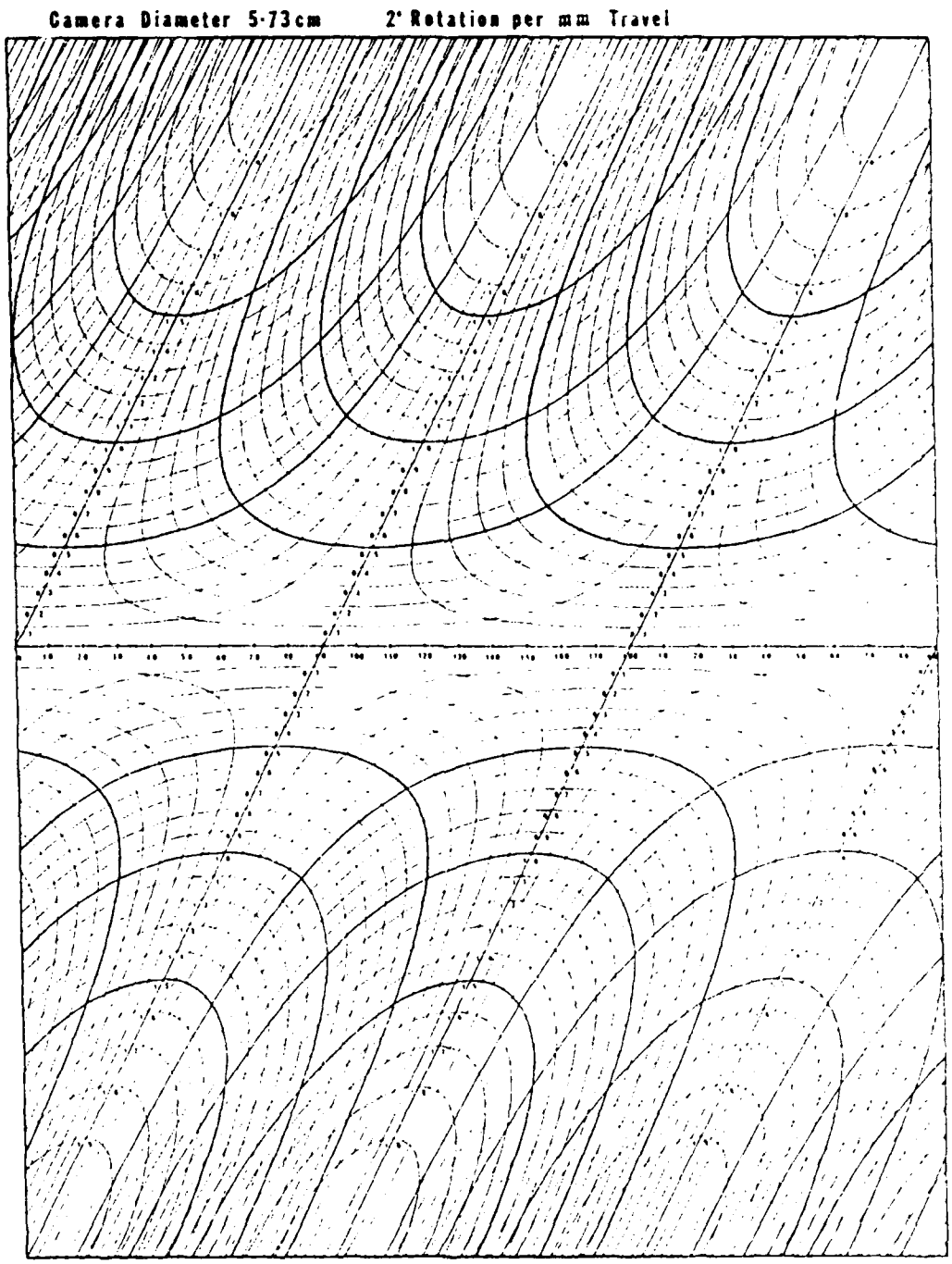

results in alignment of the spots on the film with festoon lines drawn on the template. An easy and systematic assignment of hkℓ values to the observed reflections can now be made. Indexing of the zero, first, and second-level films was accomplished in this manner. It should be noted that only the upper portion of each film was indexed as the bottom portion of each film is related to the upper portion through distorted mirror symmetry.

Upon completion of the indexing, a detailed analysis of the hkℓ values collected from each film was conducted. The object of this analysis was to determine if there were any systematic absences for a given set of reflections e.g. h0ℓ, h00, hkℓ, etc. The result of this analysis is then used to determine which symmetry elements are operating in the unit cell of a given crystal.

The analysis of the reflection indices of the target crystal revealed that in the 0k0 class of reflections a systematic absence occurred where k=2n+1 (n being an integer). Additionally, a systematic absence was observed for the h0ℓ class of reflections where h=2n+1. No other systematic absences could be detected. See Tables V through VII for a listing of experimentally observed reflections.

Based on the observed systematic absences, a search through the space groups for the monoclinic system was conducted in the International Tables For X-Ray Crystallography (24). The objective of this search was to determine whether or not the observed systematic absences coincided with the conditions for reflection of any of the

space groups in the International Tables. It should be recognized that this is a quick method for tentative identification of the space group which may or may not be fruitful.

No space group in the International Tables contained the conditions for reflection that coincided with the conditions for reflection (based on systematic absences) observed on the Weissenberg films of the target crystal. However, when the axis of rotation of the target crystal was changed from c to a and the a^* axis on the Weissenberg film changed to c^* as required, the conditions for the systematic absences of the $h0\ell$ class of reflections changes from $h=2n+1$ to $\ell=2n+1$. The conditions for reflection observed on the Weissenberg films thereafter coincided with the conditions for reflection from the $P12_1/c1$ space group as given in the International Tables. Remembering that the initial assignment of the rotation axis as c was arbitrary, no additional requirements are necessary to effect the above mentioned change. However, this does affect the sign of the upper portion of the two outermost central lattice lines on the Weissenberg films. By convention, $+c^*$ is to the left of $+b^*$. This requires that the upper portion of the left most central lattice line be positive and that of the right most central lattice line be negative. The signs of all previously tabulated reflection indices must also be changed. To verify the above conclusion, a systematic step by step process of evaluating each of the classes of

reflections observed on the Weissenberg films was conducted. The calculation of b and c required the use of the data of Table III in the following mathematical expressions:

$$b = \lambda/b^*, \quad c = \lambda/(c^* \sin\beta).$$

General reflection conditions are determined by the presence or absence of (1) centered cells, (2) glide planes, and (3) screw axes (25). Systematic absences or the lack thereof in the hkℓ class of reflections determines the centering of the unit cell. In the case of the target crystal no systematic absences were noted in the hkℓ class. This indicates a primitive unit cell, i.e. a P cell (26).

The conditions for reflection of the hk0, h0ℓ, and 0kℓ classes of reflections will determine the glide vector, orientation, and symbol of the appropriate glide plane if one is present. The conditions for systematic absence in the h0ℓ class of reflections on Weissenberg films of the target crystal was $\ell = 2n+1$. This indicates the presence of a c glide plane (27). No systematic absences were noted for the other two-dimensional classes of reflections.

The conditions for reflection in the presence of screw axes is related to the one-dimensional classes of reflection h00, 0k0, and 00ℓ (27). Systematic absences in the 0k0 class of reflections was found for k=2n+1. This indicates a 2_1 screw axis parallel to b. No systematic absences were noted for the other one-dimensional classes of reflections.

The above systematic evaluation of the reflections observed on the Weissenberg films of the target crystal verified that the crystal belongs to the $P12_1/c1$ space group, No. 14 in the International Tables For X-Ray Crystallography. With this information, the point group and diffraction symbol can be obtained from the International Tables. For the $P12_1/c1$ space group the diffraction symbol is $2/mP\text{-}2_1/c$ and the abbreviated point group symbol is $P2_1/c$ (Figure 7) (28).

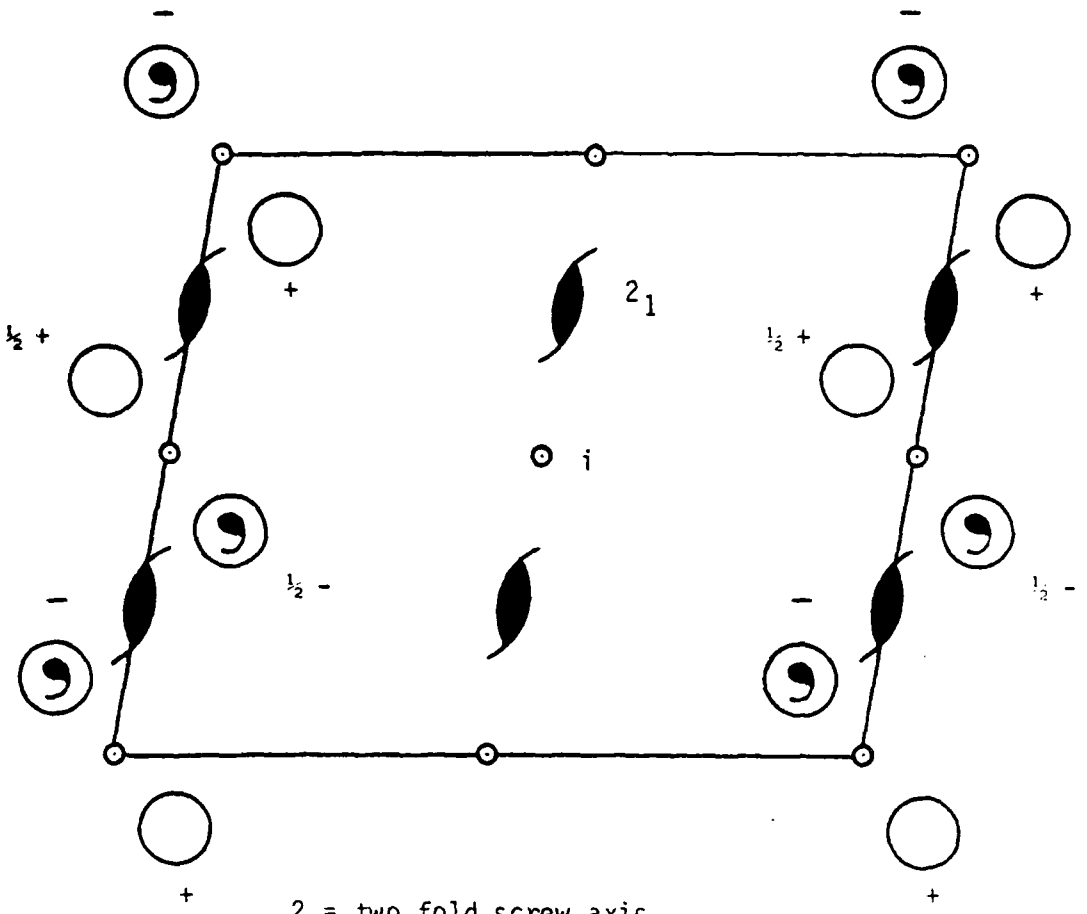

2_1 = two fold screw axis

i = center of inversion

Figure 7. Monoclinic unit cell, unique axis b, depicting two-fold screw axes with c glide and centers of inversion.

VI. Structure Determination of 5,6-Dibromonicotinic Acid

With the information now in hand, it is possible to begin the crystal structure determination process. With the equipment available, to include a microdensitometer, study of reflection intensities on Weissenberg films required for structure determination can be accomplished. This is a very long and tedious process. If a computer driven automatic diffractometer were available the required data could be collected over a much shorter period of time - days instead of months.

Through professional dialogue with Professor A. W. Cordes of the Chemistry Department at the University of Arkansas, Fayetteville, the use of an Enraf Nonius Computer Assisted Diffractometer 4, (CAD 4), was made available. Further studies to determine the crystal structure of 5,6-dibromonicotinic acid and 5-bromo-6-chloronicotinic acid were conducted on the University of Arkansas, Fayetteville campus utilizing the CAD 4 automatic diffractometer.

The target crystal was placed in a Blake Industries goniometer head and the goniometer head attached to the diffractometer. The necessity for changing goniometer heads was based on a need for a greater height adjustment to place the crystal in the x-ray beam. The crystal was then centered with respect to the x-ray beam through the use of an attached telescope.

A series of commands were given the computer to orient the crystal with respect to the x-ray beam during the exposure period. The computer then moved the crystal through

the orientation parameters given it, and thereafter collected twenty-five data points (reflections). As the CAD 4 found a reflection, it meticulously centered the reflection so as to achieve the maximum reflection intensity reading.

Upon collection of the twenty-five reflections, the computer automatically calculated a most probable unit cell, and cell constants, as well as the crystal system to which the target crystal belongs. The crystal belongs to the monoclinic system with cell edges a = 3.983 $\mathring{A}$, b = 6.270 $\mathring{A}$, c = 30.861 $\mathring{A}$, and the unique angle β = 91.92 degrees.

To create a data base from which subsequent computer programs would determine crystal structure, the crystal orientation parameters originally given the computer were expanded. Based on the symmetry of the monoclinic crystal system, a set of approximately 1500 reflections was considered sufficient for the data base. To accomplish this, the computer would search for reflections with h values from 0 to 4, k values from 0 to 7, and ℓ values from -36 to +36 out to a maximum θ value of 25 degrees. Three indices were selected to represent standard reflections during the data collection process. The computer periodically measured the intensities of these reflections to insure that the crystal had remained in the proper orientation and had not deteriorated.

After a period of approximately 38 hours, data collection was complete. The computer had searched through

1712 possible reflections over an actual exposure time of 14.2 hours.

Upon completion of intensity data collection, the several faces of the crystal were measured using the scale in the telescope attached to the diffractometer. These dimensions were provided as input to program module ABSCOR which calculated the absorption correction based on Gaussian integration formulas using the shape of the crystal and the calculated x-ray path length. The absorption data ranges from a 0.035 absorption correction for the 004 direction to 0.240 for the 211 direction with the average being 0.152. The corrected intensity data are now subjected to a series of program modules (29) which ultimately leads to the crystal structure. The first of these program modules, START, produces a set of observed structure amplitudes, i.e., $|F_{obs}|$ values from the raw intensity data upon which Lorentz, polarization, and temperature factor corrections have been applied. It is also at this point that the number and type of atoms in the molecule as well as the space group of the crystal if known is provided as input to the program. The results of the program are the calculated number of molecules in the unit cell, the x-ray density, and the linear absorption coefficient. These are respectively $z = 4$, $D_x = 2.422$ g/cm^3, and 103.7 cm^{-1} for 5,6-dibromonicotinic acid.

STDPLT produces information concerning data from measurements of the three standard reflections. This provides an indication of the loss or gain in intensity over

the total period of exposure of the crystal. As mentioned earlier, total actual exposure time was 14.2 hours with a total change in intensity of -1.5%. As part of STDPLT, program module CHORT corrects the observed structure factor amplitudes, $|F_{obs}|$, for anisotropic decay of the crystal with time using intensity standard information. The data file so created replaces the original data file.

The unit cell constants and their errors previously calculated during initial data collection are now added for consideration in the structure determination process through program module ALPHA.

The use of program module REJECT at this juncture allows for systematic absences, along with any other reflections deemed appropriate, to be rejected from consideration during structure determination calculations. Based upon the systematic absences observed on Weissenberg films, the 0k0 classes for k = 2n+1, and the h0ℓ classes for ℓ = 2n+1 were rejected. An output of those reflections rejected is also provided. Examination of the output from REJECT showed that reflections 10•13, 10•15 and 10•17 were rejected on the basis of the instruction to the computer to reject the 10ℓ reflections for which ℓ = 2n+1. This instruction was recommended because the Weissenberg films did not show these 10ℓ reflections. Other than the three specific 10ℓ reflections given above, the CAD 4 did not show other reflections from the 10ℓ class where ℓ = 2n+1. The intensities for 10•13, 10•15 and 10•17 were substantial

relative to the background intensities. This could be explained by a phenomenon that has been observed on some Weissenberg films from time to time in the experience of some workers. Some allowed and proper reflections often show smearing along a line through the reflection spot. When this happens with two neighbor spots for which the smeared "tails" overlap, a false reflection can appear. The Weissenberg films were obtained with the $Cu_{K\alpha 1}/Cu_{K\alpha 2}$ doublet having an intensity weighted average wavelength of 1.5418 Å, while the CAD 4 employs $Mo_{K\alpha 1}$ radiation having a wavelength of 0.70926 Å. Consequently, reflections with Mo radiation are confined to a range of 2θ values substantially smaller than that obtained with Cu radiation for a given crystal.

At this juncture, program module RSORT was used to sequentially resort the items in the data set.

Program module PAINT now averages the intensities of equivalent reflections. Bad data are flagged and may be omitted from averaging at this point. A new updated data file results.

DMA is a program module available to reconfigure the data file in preparation for use in program MULTAN. If no changes are desired, the existing data are put in the proper format for MULTAN.

Program module NORMAL normalizes the structure factor data. This is done by converting $|F_{obs}|$ to $|E_{obs}|$ with the expression

$$|E_{obs}|^2 = |F_{obs}|^2 / I,$$

where I is the expected intensity of a given reflection. Program output consists of a Wilson plot (30) for determination of scale and thermal correction parameters as well as normalized structure factors, E.

NORMAL leads directly into three other programs. Program MULTAN, the multi-solution direct methods program, is divided into two sections. The first section searches for phase relationships (31) and determines phase restrictions through application of space group symmetry. It defines the origin, selects reflections for phase permutations and chooses a starting point for solution of the phase relationships. The second section of MULTAN determines the phases of all reflections using the tangent formula.

The Fourier data produced by MULTAN is used by program module EXFFT to produce an E-map using the Cooley - Tukey Fourier transform. This information is automatically transferred to program module DMS which performs a peak search of the E-map. Output from DMS included a computer plot which roughly maps the asymmetric atom cluster in terms of peaks in the E-map. The number of peaks considered was decided by the program.

Program module ATOMS, designed to change or update atomic parameters, was used extensively throughout the remainder of the structure determination process. Uses include updating the list of atoms to be considered in least squares calculations, converting atoms from isotropic to

anisotropic, and updating the data file.

LSA is a program module that prepares data for use in the least squares analysis. Here an opportunity is provided to input the number of atoms on which the least squares analysis is to be conducted, select the type of weighting scheme to be used based on selections within the program, and input a scaling factor if desired.

Program module LSB performs a block diagonal least-squares refinement followed by module LSF which performs a full matrix least-squares refinement. The most significant feature of the last three modules is the production of an unweighted residual index or error factor, R, where

$$R = \Sigma|\Delta F| / \Sigma|F_{obs}| = (\Sigma||F_{obs}| - |F_{cal}||) / \Sigma|F_{obs}| .$$

It indicates the overall agreement between the observed and calculated structure factor amplitudes.

DIALOGUE F provides a series of questions allowing the user to specify parameters to be used in program module FOURIER. The type of calculation to be performed, the order of summation of the axes, and the upper and lower limits for the summation along each axis may be selected. This information is utilized by program module FOURIER to execute conventional three-dimensional Fourier calculations using the original structure factor data or the normalized structure factors from program MULTAN. The result is several files listing peak positions and map grid densities.

DIALOGUE S allows for specification of files to be used in the final determination of bond lengths and bond angles. Additionally, minimum and maximum distances to define bonds

are input. This information is used by program module SEARCH.

All data computed in the previous series of programs comes to fruition in SEARCH. Here a connectivity search through atomic coordinates is conducted in an attempt to connect atoms into molecules. Program output consists of a list of bond distances and angles, a list of atoms and peaks, a projection drawing down the crystallographic axis showing the least overlap, and a list of ghost atoms. Ghost atoms are atoms separated by less than the previously input minimum bond distance. Several runs through the least-squares programs, LSA, LSB, and LSF were required to obtain a suitable R value of 0.050. Prior to each run, program ATOMS was used to make appropriate adjustments (e.g. change number of atoms to be considered in least-squares analysis or change specific atoms from isotropic to anisotropic) to the data used. Once a suitable R value was obtained, program SEARCH was used to provide a picture of the molecule with its accompanying bond distances and bond angles. A thorough analysis of this output was conducted to insure the bond distances and angles were reasonable. Symmetry conditions were applied to the position coordinates of the asymmetric unit atoms and a sketch of the unit cell with included molecules was made. The overall result was the determination of the crystal structure for 5,6 - dibromonicotinic acid.

It should be noted that this does not represent the final refined crystal structure. However, the R value of

0.050 indicates only minor adjustments in the bond angles and distances may be required, so that the structure as a whole has been determined. In addition, the hydrogen atoms not involved in hydrogen bonding must be added and taken into consideration.

VII. Structure Determination of 5-Bromo-6-chloronicotinic Acid

The process for the structure determination of 5-bromo-6-chloronicotinic acid differed from that used for the structure determination of 5,6-dibromonicotinic acid. That is to say, no film work was done on the 5-bromo-6-chloronicotinic acid compound. As mentioned earlier the 5-bromo-6-chloronicotinic acid crystals were grown in the same manner as those for 5,6-dibromonicotinic acid. From the completion of crystal growth through the structure determination, all work was done using the Enraf Nonius CAD 4 automatic diffractometer. This portion of the structure determination of 5-bromo-6-chloronicotinic acid was carried out in the same manner as that described for 5,6-dibromonicotinic acid.

Upon collection of the twenty-five reflections for the initial data base the computer determined the crystal system of 5-bromo-6-chloronicotinic acid to be triclinic with $P\bar{1}$ space group symmetry. The cell constants found are as follows:

a = 6.090 Å	α = 97.70°
b = 9.651 Å	β = 96.02°
c = 13.724 Å	γ = 102.19°

cell volume = 774.0 $(\text{Å})^3$

The computer was then instructed to obtain a reflection data base by searching through reflections with h values form 0 to 6, k values from -11 to 11, and ℓ values from -15 to 15 out to a maximum θ value of 24 degrees.

Data were collected over an approximately 48 hour period with the actual exposure time being 22 hours. A -1.7% change in intensity over this period was determined by periodically measuring a set of predetermined standard reflections.

The absorption correction determined for 5,6-dibromonicotinic acid was obtained by actually measuring the dimensions of the crystal and applying program ABSCOR. The absorption correction for 5-bromo-6-chloronicotinic acid was determined in a different manner. The EAC program applies absorption corrections that are obtained with the PSI program. PSI is employed when the crystal has irregular shape. This latter program does two things. It maps the transmission of x-rays by the crystal over the surface of a sphere about the crystal, and then calculates absorption corrections. This resulted in a minimum absorption correction of 0.824, a maximum absorption correction of 1.00, with the average being 0.908.

As mentioned earlier, the remaining series of programs used to process the reflection data of 5-bromo-6-chloronicotinic acid are the same used for 5,6-dibromonicotinic acid. In addition to the determination of bond angles, bond distances, and atomic coordinates the following data were calculated:

number of molecules in the unit cell, Z = 4

x-ray density D_x = 2.03 g/cm^3

linear absorption coefficient = 55.5 μ^{-1}

residual index or error factor, R = 0.034

As in the case of 5,6-dibromonicotinic acid, the final refinement of the bond angle and bond distance data for the 5-bromo-6-chloronicotinic acid structure has not been conducted. It remains to "tune the hydrogen atoms" although those involved in hydrogen bonding have been located. The R value of 0.034 indicates a quite good structure determination.

VIII. Results

The results obtained from the collection of Weissenberg films, and the analysis of the geometry of diffraction of a crystal of 5,6-dibromonicotinic acid consists of the unit cell parameters, and the space group indicated by the systematic absences of the diffraction pattern. By reference to Table VIII, these results can be compared to like results for the same crystal as obtained with the automatic diffractometer.

Figure 8 constitutes a projection diagram of the structure of the unit cell for 5,6-dibromonicotinic acid. The positions of all atoms of the unit cell are indicated in Table IX, and this contains computer calculated positions for the atoms of the asymmetric unit of the unit cell. A like diagram is found in Figure 9 for 5-bromo-6-chloronicotinic acid. The positions of the atoms of the asymmetric unit in this case are in Table X along with the other atom positions obtained by application of symmetry principles.

The bond angles produced by computer calculations for 5,6-dibromonicotinic acid are in Table XI. The bond angle for 5-bromo-6-chloronicotinic acid are found in Table XII. The bond distances for the two molecules are in Tables XIII and XIV.

The distance between a pair of neighbor halogen atoms on different molecules is of interest in a number of cases. For example, the distance between Br(1) and Br(2) is one interatomic distance in a ring of eight halogen atoms in the

Figure 8. Unit cell of 5,6-dibromonicotinic acid.

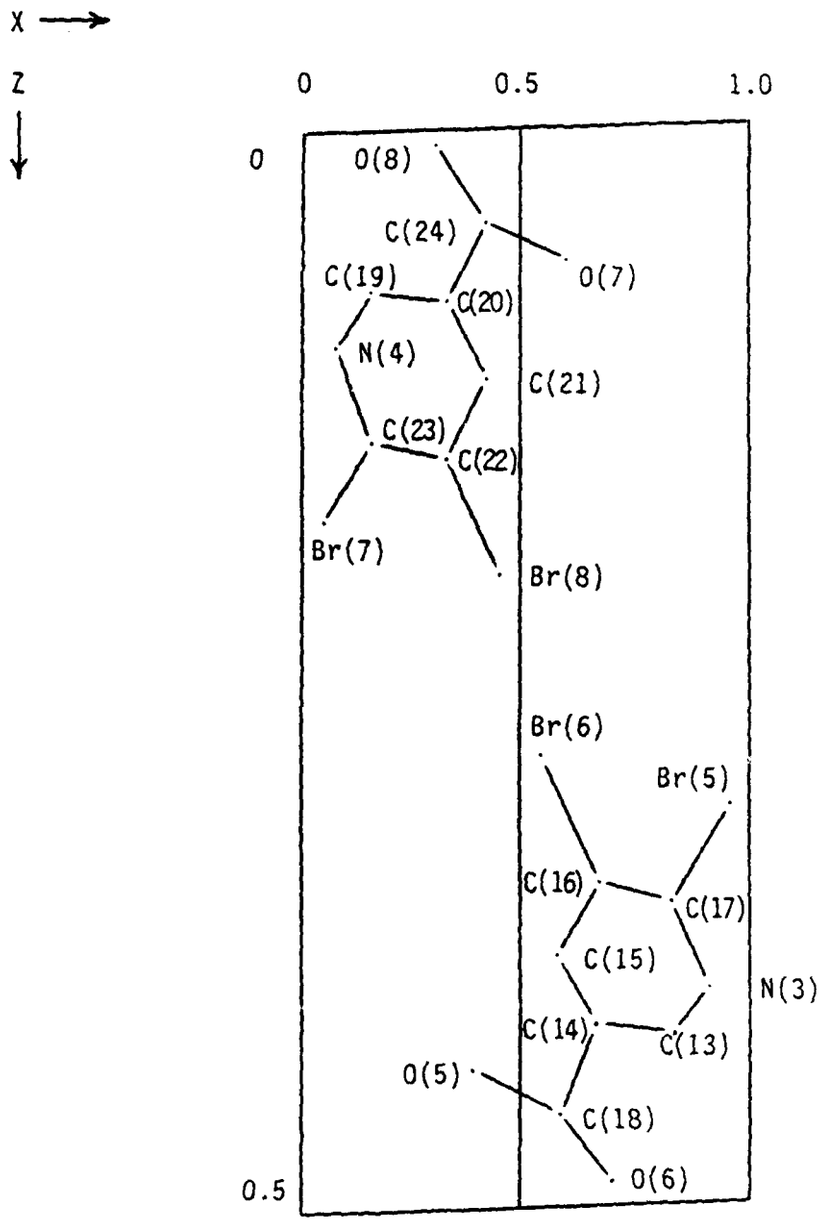

* Scale: 1cm along Z=0.5cm along X

Figure 8. Unit cell of 5,6-dibromonicotinic acid. (continued)

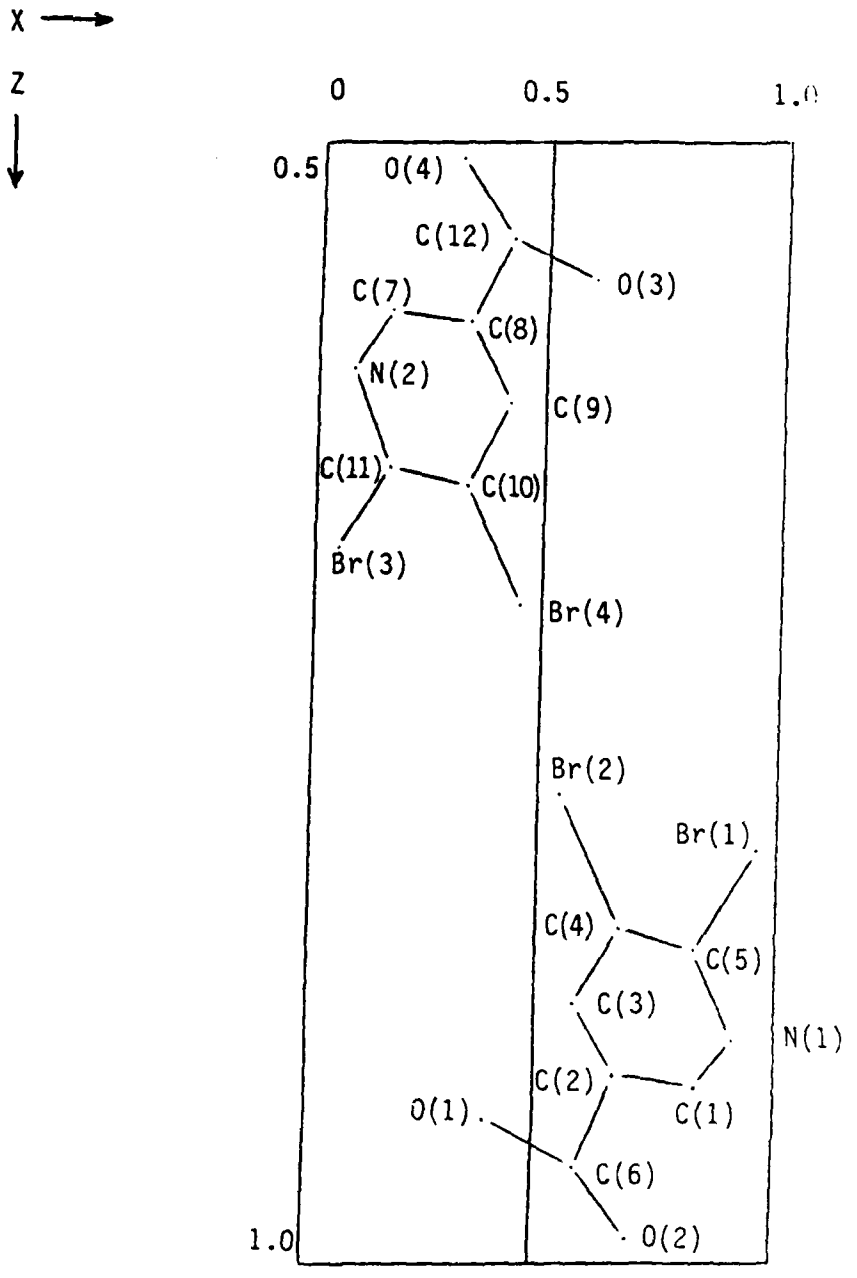

* Scale: 1 cm along Z=0.5cm along X

unit cell of 5-bromo-6-chloronicotinic acid. It is instructive to compare this distance with twice the Van der Waals radius of Br. The results from computer calculation of such distances were not on the computer printout. Accordingly, such distances were hand calculated by the means indicated here.

Let the position vector for atom Br(1) be **V**. Then $\mathbf{V} = V^i\mathbf{a}_i = 0.751\ \mathbf{a}_1 + 0.161\mathbf{a}_2 + 0.496\ \mathbf{a}_3$, where the V^i are the rectilinear or contravariant components of **V** and the $\mathbf{a}_i$ are the covariant basis vectors of the direct lattice of 5-bromo-6-chloronicotinic acid. In like manner for Br(2), $\mathbf{U} = U^j\ \mathbf{a}_j = 0.327\ \mathbf{a}_1 + 0.332\ \mathbf{a}_2 + 0.382\ \mathbf{a}_3$. Let **X** be the vector between Br(1) and Br(2). Then, $\mathbf{X} = \mathbf{U} - \mathbf{V} = -0.424\ \mathbf{a}_1 + 0.171\ \mathbf{a}_2 - 0.114\ \mathbf{a}_3$. $\mathbf{X} \cdot \mathbf{X} = X\ (X) \cos\ (\mathbf{X},\mathbf{X}) = (X)^2$, and X is the magnitude of **X**. The $a_i = |\mathbf{a}_i|$. $(X)^2 = (X^1a_1)^2 + (X^2a_2)^2 + (X^3a_3)^2 + 2(X^1X^2a_1a_2 \cos\gamma) + 2(X^1X^3a_1a_3 \cos\beta) + 2(X^2X^3a_2\ a_3 \cos\alpha) = 13.482$, and $X = 3.672$ Å.

Bondi (32) has given the Van der Waals radius for Br as 185 pm. By this, X should be 3.70 Å. The results for this and similar calculations involving other pairs of halogen atoms are given in Table XV.

IX. Discussion of Results

Of the several types of intermolecular forces which might operate in crystals of the two molecular compounds studied, it seems that permanent dipole/permanent dipole interactions, hydrogen bonding, and dispersion or Van der Waals forces would be the most important.

In the absence of experimental dipole moments, or calculations based upon tabulated bond moments, it is difficult to access the contribution of molecular polarity or the effect of polarizability of the molecule. However, an examination of the crystal structures suggests that hydrogen bonding and Van der Waals interactions are the most important.

An inspection of Figure 9, which represents the crystal structure of 5-bromo-6-chloronicotinic acid, shows a center of inversion at the center of the chosen unit cell. The number of molecules per unit cell is four, and the mode of packing of the molecules about the point of inversion at the cell center produces a ring-like array of two pairs of bromine atoms and two pairs of chlorine atoms. Van der Waals interactions among these halogens may be partially responsible for holding the molecules together. Figure 10 has a center of inversion that corresponds to one such symmetry element located at each vertical cell edge, i.e., at each a translation. The orientation of Figure 10 is not the same as that of Figure 9. The cluster of four molecules about this center of inversion appears to be due to four hydrogen bonds that are in a ring-like array of atoms. Two

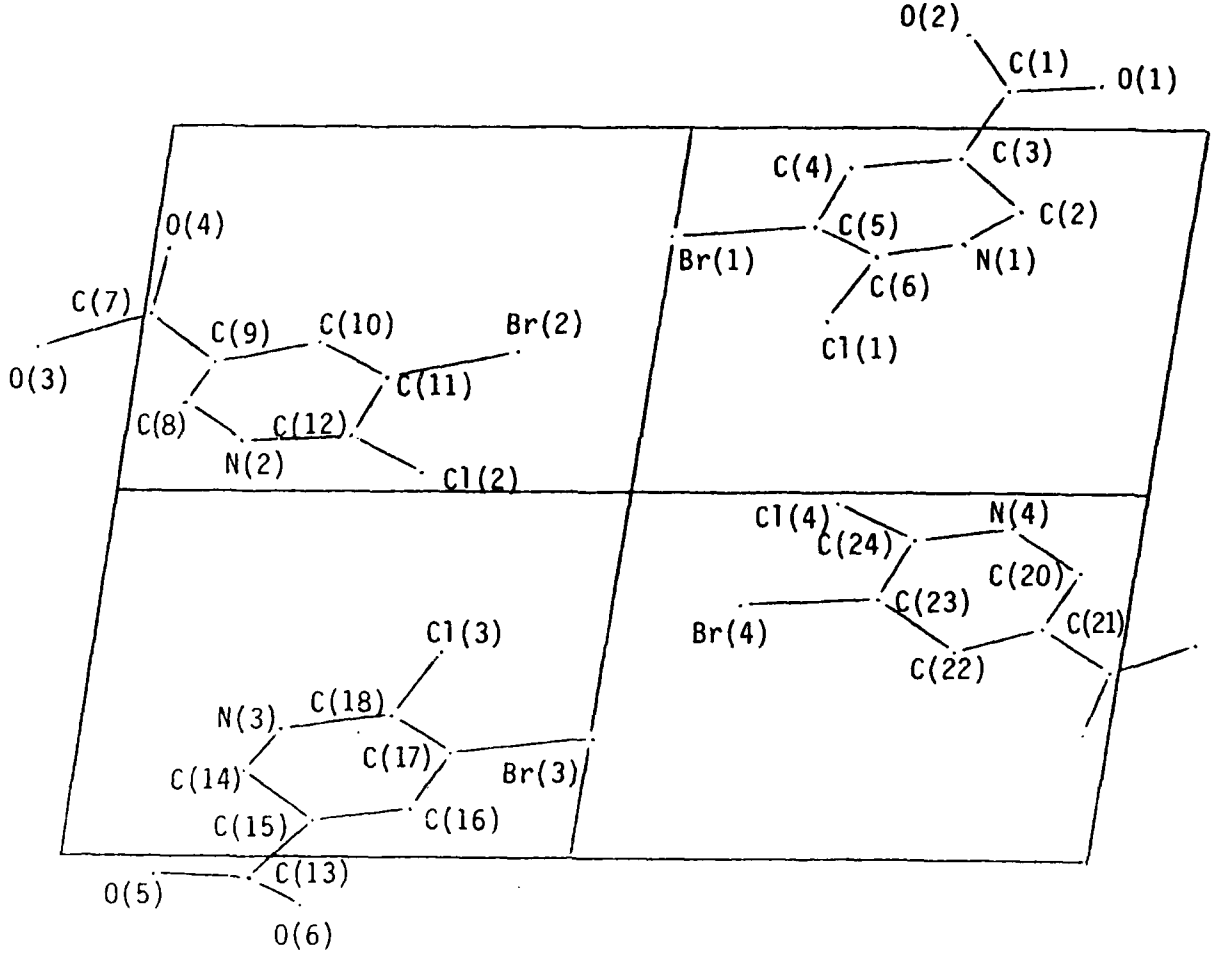

Figure 9. Unit cell of 5-bromo-6-chloronicotinic acid.

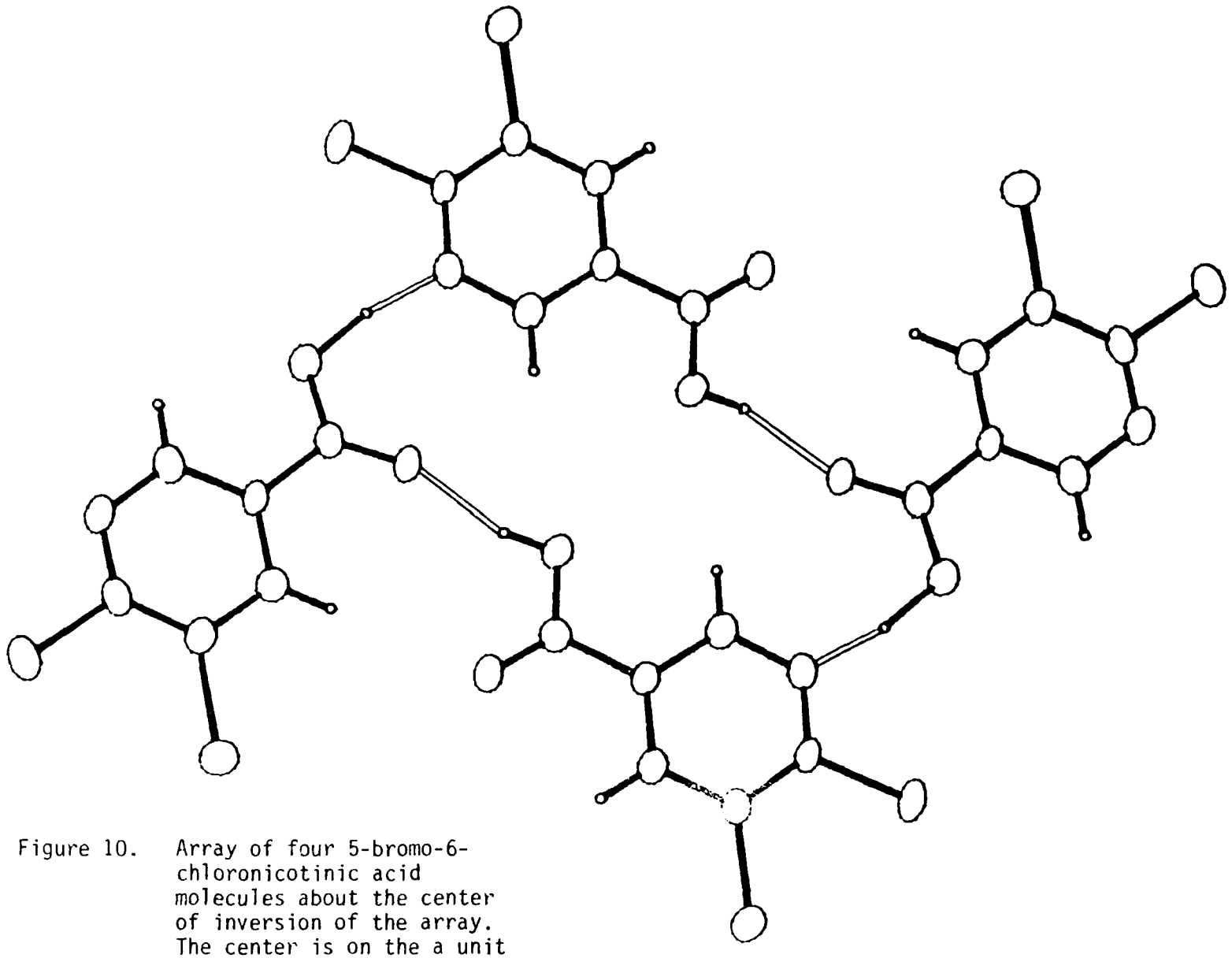

Figure 10. Array of four 5-bromo-6-chloronicotinic acid molecules about the center of inversion of the array. The center is on the a unit cell translation.

O-H---O and two O-H---N hydrogen bond types appear to be present here. In the first of these, the hydrogen atom of the OH group bonds to a carbonyl oxygen. The computer calculated value for the O---O distance is 2.619 Å. The value for the O---N distance is 2.689 Å. The first of these distances is less than 3.04 Å which is twice the Van der Waals radius of oxygen (32). The second distance is less than 3.07 Å which is the sum of the Van der Waals radii for oxygen and nitrogen (32). The proposed hydrogen bonds are present.

The ring-like array of eight halogen atoms distributed about the inversion center at the unit cell center seems to be due to Van der Waals interactions. The data of Table XV indicate that the Br(1) and Br(2) atoms, as well as the Br(3) and Br(4) atoms, are touching without overlap. On the other hand, the Cl(1) and Cl(4) pair of atoms, as well as the Cl(2) and Cl(3) pair, are well separated and probably contribute little to the mode of molecular packing. The pairs of Br atoms are weakly bound by dispersion forces.

In the unit cell of 5-bromo-6-chloronicotinic acid a= 6.09 Å. This indicates that Van der Waals interactions among molecules that are congruent along the direction of a is very weak, if present at all.

The data of Table XV indicate that in the 5,6-dibromonicotinic acid crystal, there is little to no Van der Waals interactions among pairs of Br atoms, either within a given unit cell, or between neighbor unit cells. In this

connection we note that b = 6.27 Å. On the other hand, the data show pairs of dibromonicotinic acid molecules bound together by two hydrogen bonds between the two carboxylic acid groups. See Figure 8. Here we find the O(4)---O(5) and O(3)---O(6) distances to be 2.628 Å as calculated by computer, while twice the oxygen Van der Waals radius is 3.04 Å. The proposed dimer of the dibromonicotinic acid molecule, held together by two O-H---O bonds is present.

The difference between 5,6-dibromonicotinic acid and 5-bromo-6-chloronicotinic acid seems to be a minor one from the point of view of chemical composition, molecular structure, and perhaps chemical properties. One goes from the dibromonicotinic acid molecule to the other by replacement of a Br atom with one of its neighbor cogeners. However, the crystallographic consequences of such a replacement are a substantially different crystal structure between the two substances, and a difference of hydrogen bonding and interactions among halogen atoms.

Accounting for the crystallographic difference noted above is difficult; particularly if the account is to be quantitative and based upon a mathematical analysis. For the moment, it suffices to call attention to a potential factor. Some simple calculations were performed in which the atoms Cl(1) and Cl(4) in the unit cell of 5-bromo-6-chloronicotinic acid were replaced by two bromine atoms under the following assumptions. (1) There is no other disturbance of the 5-bromo-6-chloronicotinic acid crystal structure; (2) the direction of the C(6) - Br bond is the

same as that of C(6) - Cl(1); (3) the direction of the C(24) - Br bond is the same as that of C(24) - Cl(4); (4) the two new C - Br bond lengths are the average of those for C(5) - Br(1) and C(11) - Br(2), i.e., 1.878 Å. Thereafter, the interatomic distance between the inserted Br atoms was calculated by hand. The finding was that the two Br atoms would be further apart than the two Cl atoms that were replaced, and the discrepancy between the calculated Br - Br distance and twice the Van der Waals radius of Br was greater than a similar discrepancy for the Cl(1) - Cl(4) atom pair. Consequently, one cannot account for the failure of 5,6-dibromonicotinic acid to take the structure of the 5-bromo-6-chloronicotinic acid on the basis of the inability of the replacing Br atoms to fit into the structure. What is more likely is the absence of a hydrogen bond between nitrogen and oxygen because of the presence of the larger halogen on ring position 6 in the dibromonicotinic acid molecule. Nevertheless it is premature to attempt to account for the crystal structure difference that has been found in this study. More structures for dihalonicotinic acids are required before a proper attempt can be made.

X. Future Work

A continuation of this work requires additional crystal structures of dihalonicotinic acids if one hopes to account for variations in crystal structures.

The next compounds that will be addressed will be 5-bromo-6-fluoronicotinic acid and 6-bromo-5-fluoronicotinic acid. Investigation of these is recommended by the very large tendency of fluorine to enter into hydrogen bonding. Many others should be investigated including 5,6-dichloronicotinic acid and 6-bromo-5-chloronicotinic acid. There is also the whole series of dihalonicotinic acids with halogens in the 2- and 5- positions many of which have been synthesized for the first time by Professor Setliff. Structures of other trisubstituted pyridines may also assist in development of a theory of crystal structure for dihalonicotinic acids.

Table I.

A Table of Melting Points of Trisubstituted Pyridines

Compound	m.p., °C	Reference
5-bromo-2-chloro-3-methyl-pyridine	40	(1)
2,5-dibromo-3-methylpyridine	41	(1)
5,6-dibromo-3-methylpyridine	52	(1)
5-bromo-6-fluoro-3-methyl-pyridine	54	(2)
5-bromo-2-fluoro-3-methyl-pyridine	62	(1)
5-bromo-6-chloro-3-methyl-pyridine	64	(2)
6-amino-5-bromo-3-methyl-pyridine	70	(2)
2-amino-5-bromo-3-methyl-pyridine	90	(1)
2-chloro-5-fluoronicotinamide	137	(3)
2-chloro-5-fluoronicotinic acid	145	(4)
2,5-dichloronicotinic acid	154	(5)
5,6-dichloronicotinic acid	160	(5)
6-bromo-5-chloronicotinic acid	162	(5)
5-bromo-6-chloronicotinic acid	170	(1)
5,6-dibromonicotinic acid	173	(1)
2,5-dibromonicotinic acid	174	(1)
2,5-dichloronicotinamide	176	(3)
5-bromo-2-chloronicotinic acid	179	(1)
2-chloro-5-iodonicotinamide	184	(3)
5-bromo-2-chloronicotinamide	187	(3)
5,6-dichloronicotinamide	222	(3)
5-bromo-6-chloronicotinamide	237	(3)

Table II

Calculated Repeat Distance, ζ, Along Axis of Rotation for 5,6-Dibromonicotinic Acid

A. Calculated distance between the ± 1 layer lines

estimated true distance (cm)	standard deviation	estimated probable error
1.200	1.378×10^{-3}	$\pm 1.711 \times 10^{-3}$

B. Calculated distance between the ± 2 layer lines

estimated true distance (cm)	standard deviation	estimated probable error
3.505	1.6373×10^{-3}	$\pm 2.077 \times 10^{-3}$

C. Calculated axial repeat distance

layer line	ζ	r
$\pm$ 1	0.386	3.98
$\pm$ 2	0.774	3.98

Table III

Table for Determination of Axial Repeat Distance ξ_o

For c*

2Y^	ξ	ℓ	ξ/ℓ #
11.65 $\pm 4.85 \times 10^{-4}$	0.203	4	0.050
17.45 $\pm 2.22 \times 10^{-4}$	0.305	6	0.050
20.29 $\pm 6.18 \times 10^{-4}$	0.354	7	0.050
23.28 $\pm 5.05 \times 10^{-4}$	0.406	8	0.050
29.04 $\pm 1.42 \times 10^{-4}$	0.507	10	0.050
35.01 $\pm 2.86 \times 10^{-4}$	0.611	12	0.050

For b*

2Y^	ξ	k	ξ/k #
28.25 $\pm 2.21 \times 10^{-4}$	0.493	2	0.246
59.31 $\pm 2.04 \times 10^{-4}$	1.03	4	0.257
95.31 $\pm 3.83 \times 10^{-4}$	1.66	6	0.277

^ reflection distance measurements were treated statistically using the standard students T-test.

$\xi/\ell = c^*$, $\xi/k = b^*$.

Table IV

Calculated Value of the Unique Angle for
5,6-Dibromonicotinic Acid Using the Angular Lag Method

Z"-Z'(mm)	C_2	n	ξ_o	β (degrees)
86.983	2 /mm	0.386	0.246	91.92
84.063	2 /mm	0.774	0.246	91.90
80.873	2 /mm	1.159	0.246	91.95

Table V

A Table of Experimental Reflection Indices

Zero Level Film

h = 0

h k	h k	h k	h k
2 0	4 0	6 0	0 $\bar{2}$
0 $\bar{4}$	0 $\bar{5}$	0 $\bar{6}$	0 $\bar{7}$
0 $\bar{8}$	0 $\bar{9}$	0 $\bar{10}$	0 $\bar{11}$
0 $\bar{12}$	0 $\bar{14}$	0 $\bar{15}$	0 $\bar{16}$
0 $\bar{18}$	0 $\bar{20}$	0 $\bar{22}$	0 $\bar{24}$
1 $\bar{1}$	1 $\bar{2}$	1 $\bar{3}$	1 $\bar{4}$
1 $\bar{5}$	1 $\bar{6}$	1 $\bar{7}$	1 $\bar{8}$
1 $\bar{9}$	1 $\bar{10}$	1 $\bar{11}$	1 $\bar{12}$
1 $\bar{13}$	1 $\bar{14}$	1 $\bar{15}$	1 $\bar{16}$
1 $\bar{17}$	1 $\bar{18}$	1 $\bar{19}$	1 $\bar{20}$
1 $\bar{21}$	1 $\bar{22}$	1 $\bar{23}$	1 $\bar{25}$
1 $\bar{26}$	1 $\bar{27}$	1 $\bar{28}$	1 $\bar{29}$
1 1	1 2	1 3	1 4
1 5	1 6	1 7	1 8
1 9	1 10	1 11	1 12
1 13	1 14	1 15	1 16
1 17	1 18	1 19	1 20
1 21	1 22	1 23	1 25
1 26	1 27	1 28	1 29
1 30	1 31	1 32	1 33

Table V (continued)

h	k	h	k	h	k	h	k
1	34	1	35	1	36	1	37
1	38	1	39	2	$\bar{1}$	2	$\bar{2}$
2	$\bar{3}$	2	$\bar{4}$	2	$\bar{5}$	2	$\bar{6}$
2	$\bar{7}$	2	$\bar{8}$	2	$\bar{9}$	2	$\bar{10}$
2	$\bar{11}$	2	$\bar{12}$	2	$\bar{13}$	2	$\bar{14}$
2	$\bar{15}$	2	$\bar{16}$	2	$\bar{17}$	2	$\bar{18}$
2	$\bar{19}$	2	$\bar{20}$	2	$\bar{21}$	2	$\bar{22}$
2	$\bar{23}$	2	$\bar{24}$	2	$\bar{25}$	2	$\bar{26}$
2	$\bar{27}$	2	$\bar{29}$	2	$\bar{31}$	2	1
2	2	2	3	2	4	2	5
2	6	2	7	2	8	2	9
2	10	2	11	2	12	2	13
2	14	2	15	2	16	2	17
2	18	2	19	2	20	2	21
2	22	2	23	2	24	2	25
2	26	2	27	2	29	2	30
2	31	2	33	2	34	2	35
2	36	2	37	3	$\bar{1}$	3	$\bar{2}$
3	$\bar{3}$	3	$\bar{4}$	3	$\bar{5}$	3	$\bar{6}$
3	$\bar{7}$	3	$\bar{8}$	3	$\bar{9}$	3	$\bar{10}$
3	$\bar{11}$	3	$\bar{12}$	3	$\bar{13}$	3	$\bar{15}$
3	$\bar{16}$	3	$\bar{17}$	3	$\bar{18}$	3	$\bar{19}$
3	$\bar{20}$	3	$\bar{21}$	3	$\bar{22}$	3	$\bar{23}$
3	$\bar{24}$	3	$\bar{25}$	3	$\bar{27}$	3	$\bar{28}$

Table V (continued)

h	k	h	k	h	k	h	k
3	$\bar{29}$	3	$\bar{32}$	3	1	3	2
3	3	3	4	3	5	3	6
3	7	3	8	3	9	3	10
3	11	3	12	3	13	3	14
3	15	3	16	3	17	3	18
3	19	3	20	3	21	3	22
3	23	3	24	3	25	3	27
3	28	3	29	3	31	3	32
3	34	3	35	3	36	4	$\bar{1}$
4	$\bar{2}$	4	$\bar{3}$	4	$\bar{4}$	4	$\bar{5}$
4	$\bar{6}$	4	$\bar{7}$	4	$\bar{8}$	4	$\bar{9}$
4	$\bar{10}$	4	$\bar{11}$	4	$\bar{12}$	4	$\bar{13}$
4	$\bar{14}$	4	$\bar{15}$	4	$\bar{16}$	4	$\bar{17}$
4	$\bar{19}$	4	$\bar{20}$	4	$\bar{21}$	4	$\bar{22}$
4	$\bar{23}$	4	$\bar{24}$	4	$\bar{25}$	4	$\bar{26}$
4	$\bar{28}$	4	$\bar{30}$	4	$\bar{31}$	4	$\bar{32}$
4	1	4	2	4	3	4	4
4	5	4	6	4	7	4	8
4	9	4	10	4	11	4	12
4	13	4	14	4	15	4	16
4	17	4	18	4	19	4	20
4	21	4	22	4	23	4	24
4	25	4	26	4	28	4	30
4	31	4	32	4	34	5	$\bar{1}$

Table V (continued)

h	k	h	k	h	k	h	k
5	$\bar{2}$	5	$\bar{3}$	5	$\bar{4}$	5	$\bar{5}$
5	$\bar{7}$	5	$\bar{8}$	5	$\bar{9}$	5	$\bar{10}$
5	$\bar{11}$	5	$\bar{12}$	5	$\bar{14}$	5	$\bar{15}$
5	$\bar{16}$	5	$\bar{17}$	5	$\bar{18}$	5	$\bar{19}$
5	$\bar{20}$	5	$\bar{21}$	5	$\bar{22}$	5	$\bar{23}$
5	$\bar{24}$	5	$\bar{25}$	5	$\bar{26}$	5	$\bar{27}$
5	$\bar{28}$	5	1	5	2	5	3
5	4	5	5	5	7	5	8
5	9	5	10	5	11	5	12
5	14	5	15	5	16	5	17
5	18	5	19	5	20	5	21
5	22	5	23	5	24	5	25
5	26	5	27	5	28	5	29
5	30	5	31	6	$\bar{1}$	6	$\bar{2}$
6	$\bar{3}$	6	$\bar{4}$	6	$\bar{5}$	6	$\bar{6}$
6	$\bar{7}$	6	$\bar{8}$	6	$\bar{9}$	6	$\bar{10}$
6	$\bar{11}$	6	$\bar{12}$	6	$\bar{13}$	6	$\bar{14}$
6	$\bar{15}$	6	$\bar{16}$	6	$\bar{17}$	6	$\bar{18}$
6	$\bar{19}$	6	$\bar{20}$	6	$\bar{21}$	6	$\bar{22}$
6	$\bar{24}$	6	$\bar{25}$	6	$\bar{26}$	6	1
6	2	6	3	6	4	6	5
6	6	6	7	6	8	6	9
6	10	6	11	6	12	6	13
6	14	6	15	6	16	6	17

Table V (continued)

h	k	h	k	h	k	h	k
6	18	6	19	6	20	6	21
6	22	6	24	6	25	6	26
7	$\bar{2}$	7	$\bar{3}$	7	$\bar{4}$	7	$\bar{5}$
7	$\bar{6}$	7	$\bar{8}$	7	$\bar{9}$	7	$\bar{11}$
7	$\bar{12}$	7	$\bar{13}$	7	$\bar{14}$	7	$\bar{15}$
7	$\bar{16}$	7	$\bar{17}$	7	$\bar{18}$	7	$\bar{19}$
7	2	7	3	7	4	7	5
7	6	7	8	7	9	7	10
7	11	7	12	7	13	7	14
7	15	7	16	7	17	7	18
7	19	8	$\bar{1}$	8	$\bar{2}$	8	$\bar{3}$
8	$\bar{4}$	8	$\bar{5}$	8	1	8	2
8	4	8	5	0	2	0	4
0	5	0	6	0	7	0	8
0	9	0	10	0	12	0	14
0	16	0	18	0	20	0	22
0	24	0	26	0	27	0	28
0	30	0	32	0	34	0	36
0	38	$\bar{1}$	10	$\bar{1}$	11	$\bar{1}$	12
$\bar{1}$	13	$\bar{1}$	14	$\bar{1}$	15	$\bar{1}$	16
$\bar{1}$	17	$\bar{1}$	18	$\bar{1}$	19	$\bar{1}$	20
$\bar{1}$	21	$\bar{1}$	22	$\bar{1}$	23	$\bar{1}$	25
$\bar{1}$	26	$\bar{1}$	27	$\bar{1}$	28	$\bar{1}$	29
$\bar{1}$	30	$\bar{1}$	31	$\bar{1}$	32	$\bar{1}$	33

Table V (continued)

h	k	h	k	h	k	h	k
$\bar{1}$	34	$\bar{1}$	35	$\bar{1}$	37	$\bar{1}$	38
$\bar{1}$	39	$\bar{2}$	14	$\bar{2}$	15	$\bar{2}$	16
$\bar{2}$	17	$\bar{2}$	18	$\bar{2}$	19	$\bar{2}$	20
$\bar{2}$	21	$\bar{2}$	22	$\bar{2}$	23	$\bar{2}$	24
$\bar{2}$	25	$\bar{2}$	26	$\bar{2}$	27	$\bar{2}$	29
$\bar{2}$	31	$\bar{2}$	33	$\bar{2}$	35	$\bar{2}$	36
$\bar{2}$	37	$\bar{3}$	16	$\bar{3}$	17	$\bar{3}$	18
$\bar{3}$	19	$\bar{3}$	20	$\bar{3}$	21	$\bar{3}$	22
$\bar{3}$	23	$\bar{3}$	24	$\bar{3}$	25	$\bar{3}$	27
$\bar{3}$	28	$\bar{3}$	29	$\bar{3}$	32	$\bar{3}$	34
$\bar{3}$	35	$\bar{3}$	36	$\bar{4}$	17	$\bar{4}$	19
$\bar{4}$	20	$\bar{4}$	21	$\bar{4}$	22	$\bar{4}$	23
$\bar{4}$	24	$\bar{4}$	25	$\bar{4}$	26	$\bar{4}$	28
$\bar{4}$	30	$\bar{4}$	31	$\bar{4}$	32	$\bar{4}$	34
$\bar{4}$	36	$\bar{5}$	16	$\bar{5}$	17	$\bar{5}$	18
$\bar{5}$	19	$\bar{5}$	20	$\bar{5}$	21	$\bar{5}$	22
$\bar{5}$	23	$\bar{5}$	24	$\bar{5}$	25	$\bar{5}$	26
$\bar{5}$	27	$\bar{5}$	28	$\bar{5}$	30	$\bar{5}$	31
$\bar{6}$	14	$\bar{6}$	15	$\bar{6}$	16	$\bar{6}$	17
$\bar{6}$	18	$\bar{6}$	19	$\bar{6}$	20	$\bar{6}$	21
$\bar{6}$	25	$\bar{6}$	26	$\bar{7}$	11	$\bar{7}$	12
$\bar{7}$	13	$\bar{7}$	14	$\bar{7}$	15	$\bar{7}$	16
$\bar{7}$	17	$\bar{7}$	18	$\bar{7}$	19		

Table VI

A Table of Experimental Reflection Indices

First Level Film

h = 1

h k	h k	h k	h k
1 0	2 0	3 0	5 0
6 0	7 0	0 $\bar{2}$	0 $\bar{4}$
0 $\bar{6}$	0 $\bar{8}$	0 $\bar{10}$	0 $\bar{12}$
0 $\bar{14}$	0 $\bar{16}$	0 $\bar{18}$	0 $\bar{20}$
0 $\bar{22}$	0 4	0 6	0 8
0 12	0 14	0 16	0 18
0 20	0 22	0 24	0 26
0 28	0 30	0 32	0 34
0 36	0 38	1 $\bar{1}$	2 $\bar{1}$
3 $\bar{1}$	4 $\bar{1}$	5 $\bar{1}$	7 $\bar{1}$
1 $\bar{2}$	2 $\bar{2}$	3 $\bar{2}$	5 $\bar{2}$
6 $\bar{2}$	1 $\bar{3}$	2 $\bar{3}$	3 $\bar{3}$
4 $\bar{3}$	5 $\bar{3}$	6 $\bar{3}$	7 $\bar{3}$
1 $\bar{4}$	2 $\bar{4}$	3 $\bar{4}$	4 $\bar{4}$
5 $\bar{4}$	7 $\bar{4}$	1 $\bar{5}$	2 $\bar{5}$
3 $\bar{5}$	4 $\bar{5}$	5 $\bar{5}$	6 $\bar{5}$
7 $\bar{5}$	1 $\bar{6}$	2 $\bar{6}$	3 $\bar{6}$
4 $\bar{6}$	5 $\bar{6}$	6 $\bar{6}$	7 $\bar{6}$
1 $\bar{7}$	2 $\bar{7}$	3 $\bar{7}$	4 $\bar{7}$
5 $\bar{7}$	6 $\bar{7}$	7 $\bar{7}$	1 $\bar{8}$
2 $\bar{8}$	3 $\bar{8}$	5 $\bar{8}$	6 $\bar{8}$

Table VI (continued)

h	k	h	k	h	k	h	k
7	$\bar{8}$	1	$\bar{9}$	2	$\bar{9}$	3	$\bar{9}$
4	$\bar{9}$	5	$\bar{9}$	6	$\bar{9}$	7	$\bar{9}$
1	$\bar{10}$	2	$\bar{10}$	4	$\bar{10}$	5	$\bar{10}$
6	$\bar{10}$	7	$\bar{10}$	1	$\bar{11}$	2	$\bar{11}$
3	$\bar{11}$	4	$\bar{11}$	5	$\bar{11}$	6	$\bar{11}$
7	$\bar{11}$	1	$\bar{12}$	2	$\bar{12}$	4	$\bar{12}$
5	$\bar{12}$	6	$\bar{12}$	7	$\bar{12}$	1	$\bar{13}$
2	$\bar{13}$	3	$\bar{13}$	6	$\bar{13}$	7	$\bar{13}$
1	$\bar{14}$	3	$\bar{14}$	4	$\bar{14}$	5	$\bar{14}$
6	$\bar{14}$	1	$\bar{15}$	2	$\bar{15}$	3	$\bar{15}$
5	$\bar{15}$	6	$\bar{15}$	1	$\bar{16}$	2	$\bar{16}$
3	$\bar{16}$	4	$\bar{16}$	6	$\bar{16}$	1	$\bar{17}$
2	$\bar{17}$	3	$\bar{17}$	4	$\bar{17}$	5	$\bar{17}$
6	$\bar{17}$	7	$\bar{17}$	1	$\bar{18}$	2	$\bar{18}$
3	$\bar{18}$	4	$\bar{18}$	5	$\bar{18}$	6	$\bar{18}$
7	$\bar{18}$	1	$\bar{19}$	3	$\bar{19}$	4	$\bar{19}$
5	$\bar{19}$	6	$\bar{19}$	2	$\bar{20}$	3	$\bar{20}$
4	$\bar{20}$	5	$\bar{20}$	6	$\bar{20}$	1	$\bar{21}$
2	$\bar{21}$	3	$\bar{21}$	4	$\bar{21}$	5	$\bar{21}$
6	$\bar{21}$	1	$\bar{22}$	3	$\bar{22}$	4	$\bar{22}$
6	$\bar{22}$	1	$\bar{23}$	2	$\bar{23}$	3	$\bar{23}$
4	$\bar{23}$	5	$\bar{23}$	6	$\bar{23}$	1	$\bar{24}$
2	$\bar{24}$	3	$\bar{24}$	4	$\bar{24}$	5	$\bar{24}$
6	$\bar{24}$	1	$\bar{25}$	2	$\bar{25}$	3	$\bar{25}$

Table VI (continued)

h	k	h	k	h	k	h	k
5	$\bar{2}\bar{5}$	1	$\bar{2}\bar{6}$	2	$\bar{2}\bar{6}$	3	$\bar{2}\bar{6}$
4	$\bar{2}\bar{6}$	5	$\bar{2}\bar{6}$	1	$\bar{2}\bar{7}$	2	$\bar{2}\bar{7}$
3	$\bar{2}\bar{7}$	5	$\bar{2}\bar{7}$	2	$\bar{2}\bar{8}$	3	$\bar{2}\bar{8}$
3	$\bar{2}\bar{9}$	1	1	1	2	1	3
1	4	1	5	1	6	1	7
1	8	1	9	1	10	1	11
1	12	1	13	1	14	1	15
1	16	1	18	1	19	1	20
1	21	1	22	1	23	1	24
1	25	1	26	1	27	1	28
1	29	1	30	1	31	1	32
1	33	1	34	1	35	1	36
1	37	2	1	2	2	2	3
2	4	2	5	2	6	2	7
2	8	2	9	2	10	2	11
2	12	2	13	2	14	2	15
2	16	2	17	2	18	2	21
2	22	2	23	2	24	2	25
2	26	2	27	2	28	2	30
2	31	2	32	2	33	2	35
2	37	3	1	3	2	3	3
3	4	3	5	3	6	3	7
3	8	3	9	3	10	3	11

Table VI (continued)

h k	h k	h k	h k
3 12	3 13	3 14	3 15
3 16	3 17	3 18	3 19
3 20	3 21	3 22	3 23
3 24	3 25	3 26	3 27
3 30	3 31	3 32	3 33
3 34	3 35	3 36	4 1
4 2	4 3	4 4	4 5
4 6	4 7	4 8	4 9
4 11	4 12	4 13	4 14
4 15	4 16	4 18	4 19
4 20	4 21	4 22	4 23
4 24	4 25	4 26	4 27
4 28	4 29	4 30	4 31
4 32	4 33	5 2	5 4
5 5	5 7	5 8	5 9
5 10	5 11	5 12	5 13
5 15	5 16	5 17	5 18
5 19	5 20	5 21	5 22
5 23	5 24	5 25	5 26
5 29	5 30	6 1	6 2
6 3	6 5	6 6	6 7
6 8	6 10	6 11	6 13
6 14	6 15	6 16	6 17
6 18	6 19	6 20	6 21

Table VI (continued)

h	k	h	k	h	k	h	k
6	22	6	24	6	25	7	1
7	2	7	3	7	4	7	5
7	6	7	7	7	8	7	9
7	10	7	11	7	12	7	13
7	14	7	15	7	16	7	17
7	18	$\bar{1}$	14	$\bar{1}$	15	$\bar{1}$	16
$\bar{1}$	18	$\bar{1}$	19	$\bar{1}$	20	$\bar{1}$	21
$\bar{1}$	22	$\bar{1}$	23	$\bar{1}$	24	$\bar{1}$	25
$\bar{1}$	26	$\bar{1}$	27	$\bar{1}$	28	$\bar{1}$	30
$\bar{1}$	31	$\bar{1}$	32	$\bar{1}$	33	$\bar{1}$	34
$\bar{1}$	35	$\bar{1}$	36	$\bar{1}$	37	$\bar{2}$	18
$\bar{2}$	21	$\bar{2}$	22	$\bar{2}$	23	$\bar{2}$	24
$\bar{2}$	25	$\bar{2}$	26	$\bar{2}$	27	$\bar{2}$	28
$\bar{2}$	29	$\bar{2}$	30	$\bar{2}$	31	$\bar{2}$	32
$\bar{2}$	33	$\bar{2}$	35	$\bar{2}$	37	$\bar{3}$	21
$\bar{3}$	22	$\bar{3}$	23	$\bar{3}$	24	$\bar{3}$	25
$\bar{3}$	26	$\bar{3}$	27	$\bar{3}$	28	$\bar{3}$	30
$\bar{3}$	31	$\bar{3}$	32	$\bar{3}$	33	$\bar{3}$	34
$\bar{3}$	35	$\bar{4}$	20	$\bar{4}$	21	$\bar{4}$	22
$\bar{4}$	23	$\bar{4}$	24	$\bar{4}$	25	$\bar{4}$	26
$\bar{4}$	27	$\bar{4}$	28	$\bar{4}$	29	$\bar{4}$	30
$\bar{4}$	31	$\bar{4}$	32	$\bar{4}$	33	$\bar{5}$	20
$\bar{5}$	21	$\bar{5}$	22	$\bar{5}$	23	$\bar{5}$	24
$\bar{5}$	25	$\bar{5}$	26	$\bar{5}$	28	$\bar{5}$	29

Table VI (continued)

h	k	h	k	h	k	h	k
$\bar{5}$	30	$\bar{6}$	20	$\bar{6}$	21	$\bar{6}$	22
$\bar{6}$	23	$\bar{6}$	24	$\bar{6}$	25	$\bar{7}$	20

Table VII

A Table of Experimental Reflection Indices

Second Level Film

h = 2

h	k	h	k	h	k	h	k
0	$\bar{2}$	0	$\bar{4}$	0	$\bar{6}$	0	$\bar{8}$
0	$\bar{10}$	0	$\bar{12}$	0	$\bar{16}$	0	$\bar{18}$
0	$\bar{20}$	0	$\bar{22}$	0	$\bar{24}$	0	$\bar{26}$
0	$\bar{28}$	0	$\bar{30}$	0	$\bar{32}$	0	$\bar{34}$
0	$\bar{36}$	1	0	1	$\bar{1}$	1	$\bar{2}$
1	$\bar{3}$	1	$\bar{4}$	1	$\bar{5}$	1	$\bar{6}$
1	$\bar{8}$	1	$\bar{9}$	1	$\bar{10}$	1	$\bar{11}$
1	$\bar{12}$	1	$\bar{13}$	1	$\bar{14}$	1	$\bar{15}$
1	$\bar{16}$	1	$\bar{17}$	1	$\bar{18}$	1	$\bar{19}$
1	$\bar{20}$	1	$\bar{21}$	1	$\bar{22}$	1	$\bar{23}$
1	$\bar{24}$	1	$\bar{25}$	1	$\bar{26}$	1	$\bar{27}$
1	$\bar{28}$	1	$\bar{29}$	1	$\bar{30}$	1	$\bar{31}$
1	$\bar{32}$	1	$\bar{33}$	1	$\bar{34}$	1	$\bar{35}$
2	0	2	$\bar{1}$	2	$\bar{2}$	2	$\bar{3}$
2	$\bar{4}$	2	$\bar{5}$	2	$\bar{6}$	2	$\bar{7}$
2	$\bar{8}$	2	$\bar{9}$	2	$\bar{11}$	2	$\bar{12}$
2	$\bar{13}$	2	$\bar{14}$	2	$\bar{15}$	2	$\bar{16}$
2	$\bar{17}$	2	$\bar{19}$	2	$\bar{21}$	2	$\bar{23}$
2	$\bar{24}$	2	$\bar{25}$	2	$\bar{26}$	2	$\bar{27}$
2	$\bar{29}$	2	$\bar{31}$	2	$\bar{32}$	2	$\bar{33}$

Table VII (continued)

h	k	h	k	h	k	h	k
2	$\bar{34}$	3	0	3	$\bar{1}$	3	$\bar{2}$
3	$\bar{4}$	3	$\bar{5}$	3	$\bar{6}$	3	$\bar{7}$
3	$\bar{8}$	3	$\bar{9}$	3	$\bar{10}$	3	$\bar{11}$
3	$\bar{12}$	3	$\bar{13}$	3	$\bar{14}$	3	$\bar{16}$
3	$\bar{17}$	3	$\bar{18}$	3	$\bar{19}$	3	$\bar{20}$
3	$\bar{21}$	3	$\bar{22}$	3	$\bar{24}$	3	$\bar{25}$
3	$\bar{26}$	3	$\bar{27}$	3	$\bar{28}$	3	$\bar{29}$
3	$\bar{30}$	3	$\bar{31}$	3	$\bar{32}$	4	0
4	$\bar{1}$	4	$\bar{2}$	4	$\bar{3}$	4	$\bar{4}$
4	$\bar{5}$	4	$\bar{6}$	4	$\bar{7}$	4	$\bar{8}$
4	$\bar{9}$	4	$\bar{10}$	4	$\bar{12}$	4	$\bar{13}$
4	$\bar{14}$	4	$\bar{15}$	4	$\bar{16}$	4	$\bar{17}$
4	$\bar{18}$	4	$\bar{19}$	4	$\bar{20}$	4	$\bar{22}$
4	$\bar{23}$	4	$\bar{24}$	4	$\bar{25}$	4	$\bar{26}$
4	$\bar{27}$	4	$\bar{28}$	4	$\bar{30}$	5	0
5	$\bar{1}$	5	$\bar{3}$	5	$\bar{4}$	5	$\bar{5}$
5	$\bar{6}$	5	$\bar{7}$	5	$\bar{8}$	5	$\bar{10}$
5	$\bar{12}$	5	$\bar{13}$	5	$\bar{14}$	5	$\bar{15}$
5	$\bar{16}$	5	$\bar{17}$	5	$\bar{18}$	5	$\bar{19}$
5	$\bar{20}$	5	$\bar{21}$	5	$\bar{22}$	5	$\bar{24}$
5	$\bar{25}$	6	0	6	$\bar{1}$	6	$\bar{2}$
6	$\bar{3}$	6	$\bar{4}$	6	$\bar{5}$	6	$\bar{7}$
6	$\bar{8}$	6	$\bar{9}$	6	$\bar{10}$	6	$\bar{11}$

Table VII (continued)

h	k	h	k	h	k	h	k
6	$\bar{13}$	6	$\bar{14}$	6	$\bar{16}$	6	$\bar{17}$
6	$\bar{18}$	6	$\bar{19}$	7	$\bar{2}$	7	$\bar{3}$
7	$\bar{4}$	7	$\bar{5}$	7	$\bar{6}$	7	$\bar{8}$
7	$\bar{11}$	1	1	1	2	2	1
2	3	2	4	2	5	3	1
3	2	3	3	3	4	3	5
3	6	3	7	3	8	3	9
3	10	3	11	3	12	3	13
3	14	3	15	4	2	4	3
4	4	4	5	4	7	4	8
4	9	4	10	4	11	4	12
4	13	4	15	4	16	4	17
4	18	4	20	4	21	4	22
4	23	4	24	4	26	4	27
4	28	4	29	4	30	4	31
5	1	5	2	5	3	5	4
5	5	5	7	5	8	5	9
5	10	5	11	5	12	5	13
5	14	5	15	5	16	5	17
5	18	5	19	5	20	5	21
5	22	5	23	5	24	5	25
5	26	5	27	6	1	6	2
6	3	6	4	6	6	6	8
6	9	6	11	6	12	6	13

Table VII (continued)

h	k	h	k	h	k	h	k
6	14	6	15	6	16	6	17
6	19	6	20	6	21	6	22
7	1	7	2	7	3	7	4
7	5	7	6	7	8	7	9
7	10	7	11	$\bar{1}$	0	$\bar{1}$	2
$\bar{1}$	$\bar{1}$	$\bar{1}$	$\bar{2}$	$\bar{1}$	$\bar{3}$	$\bar{1}$	$\bar{4}$
$\bar{1}$	$\bar{5}$	$\bar{1}$	$\bar{6}$	$\bar{1}$	$\bar{7}$	$\bar{1}$	$\bar{8}$
$\bar{1}$	$\bar{9}$	$\bar{1}$	$\bar{10}$	$\bar{1}$	$\bar{11}$	$\bar{1}$	$\bar{12}$
$\bar{1}$	$\bar{13}$	$\bar{1}$	$\bar{14}$	$\bar{1}$	$\bar{15}$	$\bar{1}$	$\bar{16}$
$\bar{1}$	$\bar{17}$	$\bar{1}$	$\bar{18}$	$\bar{1}$	$\bar{19}$	$\bar{1}$	$\bar{20}$
$\bar{1}$	$\bar{21}$	$\bar{1}$	$\bar{22}$	$\bar{1}$	$\bar{23}$	$\bar{1}$	$\bar{24}$
$\bar{1}$	$\bar{25}$	$\bar{1}$	$\bar{26}$	$\bar{1}$	$\bar{27}$	$\bar{1}$	$\bar{28}$
$\bar{1}$	$\bar{29}$	$\bar{1}$	$\bar{30}$	$\bar{1}$	$\bar{31}$	$\bar{1}$	$\bar{32}$
$\bar{1}$	$\bar{33}$	$\bar{1}$	$\bar{34}$	$\bar{1}$	$\bar{35}$	$\bar{2}$	$\bar{1}$
$\bar{2}$	$\bar{2}$	$\bar{2}$	$\bar{3}$	$\bar{2}$	$\bar{4}$	$\bar{2}$	$\bar{5}$
$\bar{2}$	$\bar{6}$	$\bar{2}$	$\bar{7}$	$\bar{2}$	$\bar{8}$	$\bar{2}$	$\bar{9}$
$\bar{2}$	$\bar{11}$	$\bar{2}$	$\bar{12}$	$\bar{2}$	$\bar{13}$	$\bar{2}$	$\bar{14}$
$\bar{2}$	$\bar{15}$	$\bar{2}$	$\bar{16}$	$\bar{2}$	$\bar{17}$	$\bar{2}$	$\bar{19}$
$\bar{2}$	$\bar{20}$	$\bar{2}$	$\bar{21}$	$\bar{2}$	$\bar{23}$	$\bar{2}$	$\bar{24}$
$\bar{2}$	$\bar{25}$	$\bar{2}$	$\bar{26}$	$\bar{2}$	$\bar{27}$	$\bar{2}$	$\bar{29}$
$\bar{2}$	$\bar{31}$	$\bar{2}$	$\bar{32}$	$\bar{2}$	$\bar{33}$	$\bar{2}$	$\bar{34}$
$\bar{3}$	$\bar{1}$	$\bar{3}$	$\bar{2}$	$\bar{3}$	$\bar{4}$	$\bar{3}$	$\bar{5}$
$\bar{3}$	$\bar{6}$	$\bar{3}$	$\bar{7}$	$\bar{3}$	$\bar{8}$	$\bar{3}$	$\bar{9}$
$\bar{3}$	$\bar{10}$	$\bar{3}$	$\bar{11}$	$\bar{3}$	$\bar{13}$	$\bar{3}$	$\bar{14}$

Table VII (continued)

h	k	h	k	h	k	h	k
$\bar{3}$	$\bar{16}$	$\bar{3}$	$\bar{17}$	$\bar{3}$	$\bar{18}$	$\bar{3}$	$\bar{19}$
$\bar{3}$	$\bar{20}$	$\bar{3}$	$\bar{21}$	$\bar{3}$	$\bar{22}$	$\bar{3}$	$\bar{25}$
$\bar{3}$	$\bar{26}$	$\bar{3}$	$\bar{27}$	$\bar{3}$	$\bar{28}$	$\bar{3}$	$\bar{29}$
$\bar{3}$	$\bar{30}$	$\bar{3}$	$\bar{31}$	$\bar{3}$	$\bar{32}$	$\bar{4}$	$\bar{4}$
$\bar{4}$	$\bar{5}$	$\bar{4}$	$\bar{6}$	$\bar{4}$	$\bar{8}$	$\bar{4}$	$\bar{9}$
$\bar{4}$	$\bar{10}$	$\bar{4}$	$\bar{12}$	$\bar{4}$	$\bar{13}$	$\bar{4}$	$\bar{15}$
$\bar{4}$	$\bar{16}$	$\bar{4}$	$\bar{17}$	$\bar{4}$	$\bar{18}$	$\bar{4}$	$\bar{20}$
$\bar{4}$	$\bar{22}$	$\bar{4}$	$\bar{23}$	$\bar{4}$	$\bar{24}$	$\bar{4}$	$\bar{25}$
$\bar{4}$	$\bar{26}$	$\bar{4}$	$\bar{27}$	$\bar{4}$	$\bar{28}$	$\bar{5}$	$\bar{11}$
$\bar{5}$	$\bar{12}$	$\bar{5}$	$\bar{13}$	$\bar{5}$	$\bar{14}$	$\bar{5}$	$\bar{15}$
$\bar{5}$	$\bar{16}$	$\bar{5}$	$\bar{17}$	$\bar{5}$	$\bar{18}$	$\bar{5}$	$\bar{19}$
$\bar{5}$	$\bar{20}$	$\bar{5}$	$\bar{21}$				

Table VIII

Comparison of Some Experimental Results

	5,6-Dibromo-nicotinic Acid		5-Bromo-6-chloro-nicotinic Acid
	Film	Diffractometer	Diffractometer
a	3.98 Å	3.983 Å	6.090 Å
b	6.27 Å	6.270 Å	9.651 Å
c	30.84 Å	30.861 Å	13.724 Å
α	90.00°	90.00°	97.70°
β	91.92°	91.92°	96.02°
γ	90.00°	90.00°	102.19°
cell vol	769.7 $(Å)^3$	770.3 $(Å)^3$	774.0 $(Å)^3$
Spacegroup	$P12_1/c1$	$P12_1/c1$	$P\bar{1}$
total expos. time	72 hrs	14.2 hrs	22 hrs
chg in intensity of std. refl	-	-1.5%	-1.7%
Z	-	4	4
formula weight	-	280.914	236.5
density, D_x	-	2.422 gm/cm^3	2.03 gm/cm^3
absorption coefficient, linear	-	103.67 cm^{-1}	55.5 cm^{-1}

Table VIII (continued)

absorption correction:			
min	-	0.035 cm^{-1}	0.824 cm^{-1}
max	-	0.240 cm^{-1}	1.00 cm^{-1}
avg	-	0.157 cm^{-1}	0.908 cm^{-1}
R	-	0.050	0.034
total # of refl collected	3536	1712	2674
# of refl rejected	0	153	261
# of refl used in analysis	1793	1348	2413

Table IX

Atom Position * Coordinates for 5,6-Dibromonicotinic Acid

Atom	x	y	z
Br(1)	0.947	0.155	0.818
Br(2)	0.550	0.613	0.787
O(1)	0.403	0.960	0.944
O(2)	0.704	0.775	0.992
N(1)	0.912	0.319	0.899
C(1)	0.841	0.461	0.931
C(2)	0.675	0.653	0.919
C(3)	0.583	0.699	0.877
C(4)	0.668	0.551	0.845
C(5)	0.832	0.366	0.859
C(6)	0.595	0.800	0.956
---	---	---	---
Br(3)	0.053	-0.346	0.682
Br(4)	0.450	0.113	0.713
Br(5)	0.947	1.346	0.318
Br(6)	0.549	0.887	0.287
Br(7)	0.053	0.846	0.182
Br(8)	0.450	0.387	0.213
Br(9)	-0.053	1.346	0.318
O(3)	0.597	0.460	0.556
O(4)	0.296	0.275	0.508
O(5)	0.403	0.539	0.444
O(6)	0.704	0.726	0.492
O(7)	0.597	0.039	0.056
O(8)	0.296	0.226	0.008
N(2)	0.088	-0.181	0.601
N(3)	0.912	1.181	0.399
N(4)	0.088	0.681	0.101
C(7)	0.159	-0.390	0.569
C(8)	0.325	0.153	0.581
C(9)	0.417	0.199	0.623
C(10)	0.332	0.051	0.655
C(11)	0.168	-0.134	0.641
C(12)	0.405	0.300	0.544
C(13)	0.841	1.039	0.431
C(14)	0.675	0.848	0.419
C(15)	0.583	0.801	0.377
C(16)	0.668	0.949	0.345
C(17)	0.832	1.134	0.359
C(18)	0.595	0.699	0.456
C(19)	0.159	0.539	0.069
C(20)	0.325	0.348	0.081
C(21)	0.417	0.301	0.123
C(22)	0.332	0.449	0.155
C(23)	0.168	0.634	0.141
C(24)	0.405	0.199	0.044

* Atoms above the dashed line make up the asymmetric unit.

Table X

Atom Position * Coordinates for 5-Bromo-6-chloronicotinic Acid

Atom	x	y	z
Br(1)	0.751	0.162	0.496
Br(2)	0.328	0.332	0.382
Cl(1)	0.451	0.283	0.659
Cl(2)	-0.062	0.488	0.299
O(1)	1.131	-0.039	0.896
O(2)	1.237	-0.088	0.747
O(3)	0.427	0.296	-0.081
O(4)	0.400	0.182	0.023
N(1)	0.671	0.179	0.792
N(2)	0.054	0.442	0.125
C(1)	1.123	-0.033	0.799
C(2)	0.825	0.106	0.828
C(3)	0.954	0.045	0.764
C(4)	0.929	0.059	0.664
C(5)	0.775	0.133	0.630
C(6)	0.651	0.191	0.696
C(7)	0.468	0.260	0.006
C(8)	0.175	0.390	0.056
C(9)	0.338	0.316	0.081
C(10)	0.386	0.297	0.178
C(11)	0.264	0.352	0.246
C(12)	0.098	0.420	0.214
---	---	---	---
Br(3)	0.249	0.848	0.504
Br(4)	0.672	0.668	0.618
Cl(3)	0.549	0.717	0.341
Cl(4)	1.062	0.512	0.701
O(5)	-0.131	1.039	0.104
O(6)	-0.237	1.088	0.253
O(7)	0.573	0.704	1.081
O(8)	0.600	0.818	0.977
N(3)	0.329	0.821	0.208
N(4)	0.946	0.558	0.875
C(13)	-0.123	1.033	0.201
C(14)	0.175	0.894	0.172
C(15)	0.046	0.955	0.236
C(16)	0.071	0.941	0.336
C(17)	0.225	0.867	0.370
C(18)	0.349	0.809	0.304
C(19)	0.532	0.740	0.994
C(20)	0.825	0.610	0.944
C(21)	0.666	0.684	0.919
C(22)	0.614	0.703	0.822
C(23)	0.736	0.648	0.754
C(24)	0.902	0.580	0.786

* Atoms above the dashed line make up the asymmetric unit.

Table XI

Bond Angles for 5,6-Dibromonicotinic Acid

Bond	Angle (degrees)
C(1)-N(1)-C(5)	119.1
N(1)-C(1)-C(2)	119.3
C(1)-C(2)-C(3)	121.3
C(2)-C(3)-C(4)	117.6
Br(2)-C(4)-C(3)	118.4
Br(1)-C(5)-N(1)	115.0
Br(2)-C(4)-C(5)	124.4
Br(1)-C(5)-C(4)	119.5
O(1)-C(6)-O(2)	124.0
C(1)-C(2)-C(6)	117.3
O(1)-C(6)-C(2)	113.5
C(3)-C(2)-C(6)	121.4
C(3)-C(4)-C(5)	117.1
N(1)-C(5)-C(4)	125.5
O(2)-C(6)-C(2)	122.5

Table XII

Bond Angles for 5-Bromo-6-chloronicotinic Acid

Bond	Angle (degrees)
C(2)-N(1)-C(6)	118.6
O(1)-C(1)-O(2)	124.1
O(2)-C(1)-C(3)	122.8
N(1)-C(2)-C(3)	120.1
C(1)-C(3)-C(2)	120.9
C(3)-C(4)-C(5)	119.0
Br(1)-C(5)-C(4)	119.8
Cl(1)-C(6)-N(1)	114.9
O(1)-C(1)-C(3)	113.1
C(1)-C(3)-C(4)	118.7
Br(1)-C(5)-C(6)	122.2
Cl(1)-C(6)-C(5)	120.9
C(2)-C(3)-C(4)	120.3
C(4)-C(5)-C(6)	117.9
N(1)-C(6)-C(5)	124.2
C(8)-N(2)-C(12)	117.7
O(3)-C(7)-O(4)	122.6
N(2)-C(8)-C(9)	121.7
C(7)-C(9)-C(8)	120.9
C(9)-C(10)-C(11)	117.3
Br(2)-C(11)-C(10)	119.2
Cl(2)-C(12)-N(2)	115.2
O(3)-C(7)-C(9)	114.4
C(7)-C(9)-C(10)	119.1
Br(2)-C(11)-C(12)	121.7
Cl(2)-C(12)-C(11)	120.7
O(4)-C(7)-C(9)	123.0
C(8)-C(9)-C(10)	120.1
C(10)-C(11)-C(12)	119.1
N(2)-C(12)-C(11)	124.0

Table XIII

Bond Distances for 5,6-Dibromonicotinic Acid

Bond	Distance (Å)
Br(2)-C(4)	1.873
Br(1)-C(5)	1.910
O(1)-C(6)	1.308
O(2)-C(6)	1.204
C(5)-N(1)	1.286
N(1)-C(1)	1.360
C(1)-C(2)	1.407
C(6)-C(2)	1.495
C(2)-C(3)	1.376
C(3)-C(4)	1.403
C(4)-C(5)	1.395
Br(6)-Br(8)	3.891
Br(7)-Br(9)	5.282
O(4)-O(5)	2.628

Table XIV

Bond Distances for 5-Bromo-6-chloronicotinic Acid

Bond	Distance (Å)
C(1)-O(1)	1.320
C(2)-N(1)	1.368
N(1)-C(6)	1.323
C(1)-O(2)	1.201
C(1)-C(3)	1.492
C(2)-C(3)	1.399
C(3)-C(4)	1.382
C(4)-C(5)	1.383
Br(1)-C(5)	1.868
Cl(1)-C(6)	1.729
C(5)-C(6)	1.390
C(7)-O(3)	1.309
O(4)-C(7)	1.224
C(8)-N(2)	1.351
N(2)-C(12)	1.312
C(8)-C(9)	1.386
C(7)-C(9)	1.489
C(9)-C(10)	1.384
C(10)-C(11)	1.380
Br(2)-C(11)	1.889
Cl(2)-C(12)	1.735
C(12)-C(11)	1.382
O(3)-N(1)	2.689
O(1)-O(4)	2.619

Table XV

A table of Calculated Interhalogen Distances

A. 5-Bromo-6-chloronicotinic Acid

Halogen pair	Calculated Interatomic Distance (Å)	Twice the Van der Waals Radius (38)
Br(1)-Br(2)	3.672	3.70
Cl(1)-Cl(4)	3.837	3.50

B. 5,6-Dibromonicotinic Acid

Halogen pair	Calculated Interatomic Distance (Å)	Twice the Van der Waals Radius (38)
Br(6)-Br(8)	3.891	3.70
Br(7)-Br(9)	5.282	3.70

Bibliography

1. Setliff, F.L., J. Chem. Eng. Data, 15, 590 (1970).

2. Link, W.J., Borne, R.F., and Setliff, F.L., J. Heterocyclic Chem., 4, 641 (1967).

3. Setliff, F.L., and Hill, J.F., Organic Preparations and Procedures International, 12, 259 (1980).

4. Setliff, F.L., and Rankin, G.O., J. Chem. Eng. Data, 17, 515 (1972).

5. Setliff, F.L., and Lane, J.E., J. Chem. Eng. Data, 21, 246 (1976).

6. Setliff, F.L., and Greene, J.S., J. Chem. Eng. Data, 23, 96 (1978).

7. Hamilton, W.C., and Ibers, J.A., "Hydrogen Bonding In Solids Methods of Molecular Structure Determination," W.A. Benjamin, Inc., New York, Amsterdam, 1968.

8. Kitaigorodskii, A.I., "Organic Chemical Crystallography," Consultants Bureau, New York, 1961.

9. Laing, M., South African J. Sci., 71, 171 (1975).

10. International Centre for Diffraction Data, Powder Diffraction File, Pattern 37-1982 (5,6-Dibromonicotinic Acid), September, 1987; Ibid., Pattern 37-1977 (5-Bromo-6-chloronicotinic Acid), September 1987.

11. Ito, T., "X-ray Studies on Polymorphism," Maruzen Co., LTD., Tokyo, 1950, pp. 187-228.

12. NBS * AIDS 83 Manual, International Centre for Diffraction Data, July 1, 1987.

13. Stout, B. and Jensen, L., "X-ray Structure Determination A Practical Guide," Macmillan Publishing Co., Inc., New York, 1968, p. 66.

14. Ibid., p. 73.

15. Ibid., p. 97.

16. Ibid., p. 96.

17. Sands, D.E., "Introduction to Crystallography," W.A. Benjamin, Inc., New York, Amsterdam, 1969, Appendix 2.

18. Buerger, M.J., "X-ray Crystallography An Introduction to the Investigation of Crystals by Their Diffraction of Monochromatic X-Radiation," John Wiley & Sons, Inc. New York, London, Sydney, 1942, Chapter 6.

19. Loc. cit., Stout, B., Jensen, L., pp. 94-95.

20. Loc. cit., Stout, B., Jensen, L., pp. 98-110.

21. Loc. cit., Stout, B., Jensen, L., pp. 117-120.

22. Loc. cit., Stout, B., Jensen, L., pp. 110-115.

23. Loc. cit., Buerger, M.J., pp. 377-381.

24. "International Tables for X-Ray Crystallography," Volume I, Norman F.M. Henry and Kathleen Lonsdale (Editors), The Kynoch Press, Birmingham, 1969, Sec. 4.3.

25. "International Tables for Crystallography," Volume A, Second revised edition, Theo Hahn (Editor), D. Riedel Publishing Company, Dordrecht, Boston, Lancaster, Tokyo, 1987, Sec. 7.

26. Ibid., Sec. 2.13.1.

27. Ibid., Sec. 2.13.2.

28. Ibid., Sec. 4.43.

29. B.A. Frenz and Associates, Inc., College Station, Texas 77840 and Enraf Nonius, Delft, Holland.

30. Loc. cit., Stout, B., Jensen, L., pp. 205-211.

31. Loc. cit., B.A. Frenz, p. 208.

32. Bondi, A., J. Phys. Chem., 68, 441 (1964).

Vita

Major Clarence A. Everly, Jr. [redacted] He holds a Bachelor of Science Degree in Chemistry from North Georgia College at Dahlonega, Georgia, with a minor in Physics.

The author's military career started while in college. He finished his college education as the Distinguished Military Graduate, and was comissioned as an Army officer in May 1976. Thereafter, he went on to pursue a military career at Fort Benning, where he was named Distinguished Honor Graduate from the Infantry Officer Advanced Course. Major Everly has held various military positions including Company Executive Officer, Adjutant to the 82nd Airborne Division, Brigade Operations Officer to the Fourth Brigade of the Fourth Infantry Division. His most recent assignment has been that of Assistant Professor of Military Science to the Reserve Officer's Training Corps at the University of Arkansas at Little Rock.

Major Everly holds the Meritorious Service Medal (twice awarded), the Army Commendation Medal, the Army Achievement Medal, the Overseas Service Medal, the Army Service Medal, the Expert Infantryman's Badge, the Master Parachutist Badge, and the Ranger Tab.